JOURNAL
OF
GEOMAGNETISM
AND
GEOELECTRICITY

VOL. IX NO. 4

SOCIETY
OF
TERRESTRIAL MAGNETISM AND ELECTRICITY
OF
JAPAN

1957
KYOTO

JOURNAL OF GEOMAGNETISM AND GEOELECTRICITY

EDITORIAL OFFICE: Society of Terrestrial Magnetism and Electricity of Japan, Geophysical Institute, Kyoto University, Kyoto, Japan

The fields of interest of this quarterly Journal are as follows:

Terrestrial Magnetism	Aurora and Night Airglow
Atmospheric Electricity	The Ozone Layer
The Ionosphere	Physical States of the Upper Atmosphere
Radio Wave Propagation	Solar Phenomena relating to the Above Subjects
Cosmic Rays	Electricity within the Earth

The text should be written in English, German or French. The price is set as 1 dollar per number. We hope to exchange this Journal with periodical publications of any kind in the field of natural science.

The Editors

Magnetic Properties of $TiFe_2O_4$–Fe_3O_4 System and Their Change with Oxidation*

By Syun-iti AKIMOTO

Geophysical Institute, Tokyo University,

Takashi KATSURA and Minoru YOSHIDA

Laboratory of Analytical Chemistry and Geochemistry, Tokyo Institute of Technology.

(Read Oct. 9, 1957; Received July 1, 1958)

Abstract

A series of solid solution $x TiFe_2O_4 \cdot (1-x)Fe_3O_4$ was synthesized by ceramic method over a whole range of the composition, $1 \geqq x \geqq 0$. Changes of the Curie point, saturation moment and the lattice parameter with the composition were examined. Generalized titanomagnetite having some vacant site in the structure normally occupied in a spinel was also prepared by oxidizing the $TiFe_2O_4$–Fe_3O_4 solid solution series. The region within which the spinel structure can be in existence as a single phase was settled in a $FeO-Fe_2O_3-TiO_2$ system. An equal lattice parameter line, equal Curie point line and equal saturation moment line for the generalized titanomagnetite were drawn on the FeO–Fe_2O_3–TiO_2 system.

1. Introduction

It has been established from recent study on the ferromagnetic minerals contained in rocks that the chemical composition of the natural titanomagnetite with spinel structure does not always accord with $TiFe_2O_4$–Fe_3O_4 join but in most cases deviates from this join towards $TiFeO_3$–Fe_2O_3 join side and occasionally FeO side in a FeO–Fe_2O_3–TiO_2 system. As long as we deal with these natural specimens, it may be very probable that the various magnetic properties are considerably scattered with respect to the calculated $TiFe_2O_4$ content which was tentatively used in the previous paper as a measure representative of their chemical composition (Akimoto; 1954, 1955).

It is indispensable for interpreting correctly the magnetic properties of these natural titanomagnetites to perform a systematic study on the synthetic titanomagnetites which were prepared under the known physico-chemical condition. Several magneto-chemical studies along this line have already been reported by Ernst (1943), Pouillard (1950), Chevallier and Girard (1950), Kawai, Kume and Sasajima (1954), and Chevallier, Bolfa and Mathieu (1955). The data obtained hitherto by these authors are still unsatisfactory for applying to the interpretation of the magnetic properties of natural titanomagnetites. Pouillard's synthetic titanomagnetites are limited to the solid solution $x TiFe_2O_4 \cdot (1-x)Fe_3O_4$ of $TiFe_2O_4$ and Fe_3O_4 over a range of $0.42 > x > 0$. He synthesized

* Contribution from Division of Geomagnetism and Geoelectricity, Geophysical Institute, Tokyo University. Series II. No. 78.

his specimens either by heating mixture of TiO_2 and Fe_3O_4 in an evacuated furnace for one hour at 900°C or by reducing mixture of TiO_2 and Fe_2O_3 with hydrogen gas for two hours at 450°C. In each case other phases were also formed and he estimated the molecular percentages of $TiFe_2O_4$ by applying the law of Vegard (linear relation between crystal parameter and molecular composition). Therefore, as Nicholls (1955) pointed out in his review on rock-forming ferromagnetic minerals, there remain still some ambiguities upon the chemical composition on his specimens. Although Kawai, Kume and Sasajima have reported that they succeeded in extending the range of synthetic spinels to $x=0.8$ with the aid of usual ceramic method, they do not give any detailed description on the way in which the composition of the synthetic specimen was determined.

On the other hand, very little work has been done with respect to the magnetochemistry on the cubic solid solutions between $TiFe_2O_4$–Fe_3O_4 join and $TiFeO_3$–Fe_2O_3 join. The only information available is the work carried out on $TiFeO_3$–Fe_3O_4 solid solution series by Chevallier and Girard (1950) and Chevallier, Bolfa and Mathieu (1955). They have synthesized cubic solid solutions intermediate between Fe_3O_4 and $TiFeO_3$ up to 37 molecular percent of $TiFeO_3$ by means of a borax method.

Under the circumstances, we intended to extend the studies hitherto made to the more broad region between $TiFe_2O_4$–Fe_3O_4 join and $TiFeO_3$–Fe_2O_3 join. As the first step of the study we synthesized the solid solution $x TiFe_2O_4 \cdot (1-x)Fe_3O_4$ over a whole range of the composition. Then we synthesized the cubic solid solution in the concerned region by oxidizing the $TiFe_2O_4$–Fe_3O_4 series specimens. The particular interests shown in this paper are related to the following two:

(1) The one is to settle the region on the FeO–Fe_2O_3–TiO_2 system, within which the spinel structure can be in existence as a single phase.

(2) The other is to draw an equal lattice parameter line, equal Curie point line or equal saturation moment line on the FeO–Fe_2O_3–TiO_2 ternary system.

2. Preparation of $TiFe_2O_4$–Fe_3O_4 Solid Solution Series

The specimens dealt with in the present study were prepared by the sintering procedure generally used in the ceramics. A fine powder mixture of pure Fe_2O_3, TiO_2 and electrolytic iron in the desired proportion, sealed in a silica tube evacuated approximately to 10^{-3} mmHg, was quenched from 1150°C after being maintained at this temperature for six hours.

Twenty specimens were prepared by this method over the whole range of $1 \geq x \geq 0$. The chemical composition of the synthesized specimen is plotted by full circles on the FeO–Fe_2O_3–TiO_2 diagram in Fig. 1 and is given in Table I.

Analysis by means of the "Norelco" X-ray diffractometer shows that these specimens are generally composed of a single phase having the spinel structure. No trace of the ilmenite-hematite series could be found except the specimen S 2–4. Even in this specimen the amounts of the ilmenite-hematite series minerals were estimated to be less than ten percent from the careful examination of the diffraction chart.

Lattice parameters of all synthetic specimens determined from the X-ray analysis are also given in Table I. In Fig. 2 the lattice parameter is plotted against the $TiFe_2O_4$ content x, which was tentatively determined from the data of chemical analysis as a mean value of the following two values of x derived from different assumptions: the one is based on the assumption that all the titanium oxides are involved into the ulvöspinel ($TiFe_2O_4$), the other being based on the assumption that all the ferric oxides are attributed to magnetite (Fe_3O_4). As will be seen in Fig. 2 and Table I, it was established that a solid solution $x TiFe_2O_4 \cdot (1-x)Fe_3O_4$ of spinel structure can be formed continuously throughout the whole range of $1 \geqq x \geqq 0$. The lattice parameter varies almost linearly with the composition from about 8.39 Å of Fe_3O_4 to 8.53 Å of $TiFe_2O_4$.

3. Oxidation of $TiFe_2O_4$–Fe_3O_4 Solid Solution Series

Some experimental work on the oxidation of titanomagnetite has been carried out by Nagata and Ozima (1955) in connection with the interpretation of a particular phenomenon of thermoremanent magnetism, i.e. anomalous increase of thermoremanent magnetism. They suggested that a material having spinel structure could be remained

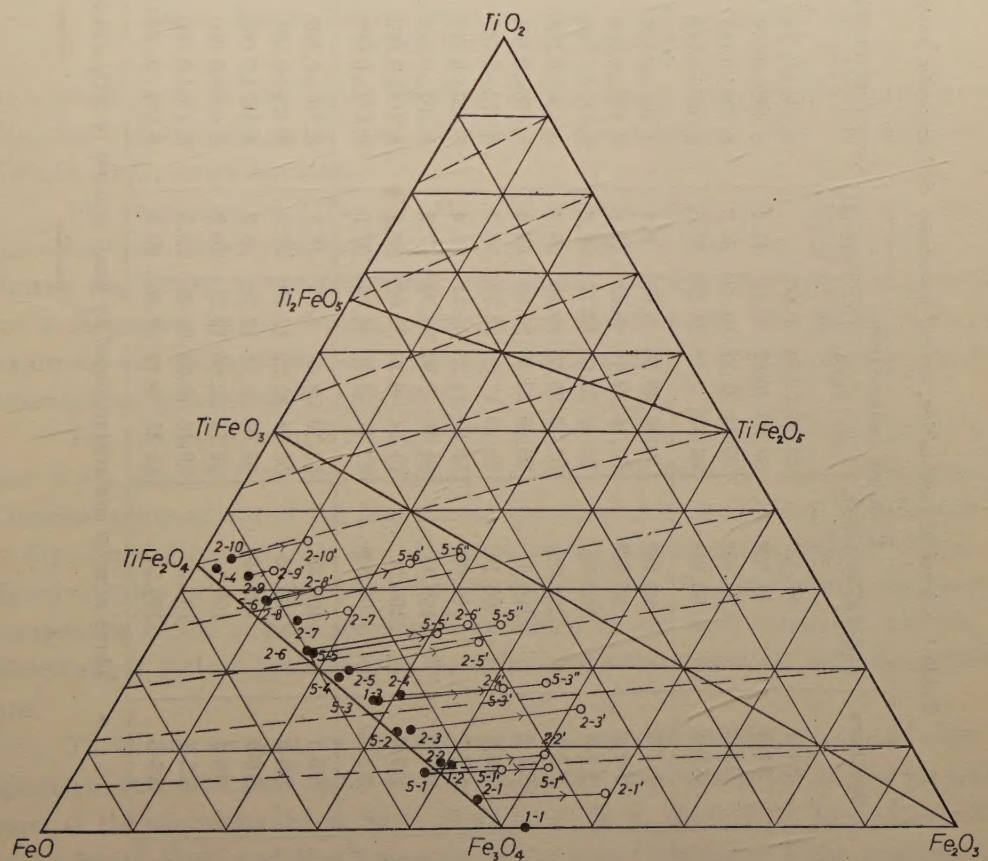

Fig. 1 Chemical composition of synthetic titanomagnetites, represented on a FeO–Fe_2O_3–TiO_2 ternary diagram in mol. percent.
Broken line: theoretical reduction-oxidation line.

Table I *Chemical composition, crystal parameter and magnetic properties of $TiFe_2O_4$–Fe_3O_4 solid solution series.*

Specimen	Chemical composition					Crystal parameter, a (Å)	Curie point, Θ (°C)	Saturation moment, σ (e.m.u./gr.)		Estimated saturation moment at 0°K (μ_B)
	$FeO+Fe_2O_3+TiO_2$ wt%	FeO	Fe_2O_3	TiO_2 mol%	$TiFe_2O_4$ mol%			at room temp.	at 80°K	
S1-1	97.13*	47.16	52.84	0.00		8.394±0.001	580	93		4.02
S1-2	97.32*	51.30	40.57	8.13	15.4	8.409±0.001				
S1-3	98.62*	55.84	27.77	16.39	37.3	8.438±0.001	330	49		2.17
S1-4	93.97*	64.59	2.18	33.23	95.8	8.527±0.000	−105		4	0.16
S2-1	95.69*	50.46	45.86	3.68	6.4	8.402±0.001	550	85		3.80
S2-2	96.91*	52.16	39.41	8.43	16.8	8.416±0.001	480	76		3.38
S2-3	100.50	53.27	33.99	12.74	26.3	8.427±0.001	420	60		2.63
S2-4	100.03	52.49	30.55	16.96	35.4	8.436±0.001	400	44		2.01
S2-5	100.57	56.65	23.35	20.00	46.6	8.456±0.001	280	48		2.16
S2-6	100.10	59.73	17.55	22.72	56.7	8.473±0.001	160	31	35	1.42
S2-7	100.69	58.93	14.53	26.54	65.4	8.486±0.001	110	19	25	1.05
S2-8	100.45	61.07	9.97	28.96	77.8	8.504±0.001	47		16	0.64
S2-9	100.56	61.54	6.39	32.07	88.1	8.519±0.002	−61		9	0.36
S2-10	98.80*	62.41	3.26	34.33	97.2	8.527±0.002				
S5-1	100.38	55.12	38.02	6.86	16.2	8.416±0.002	490			
S5-2	100.45	55.56	32.22	12.22	27.2	8.428±0.001	420			
S5-3	100.22	55.68	28.12	16.20	36.2	8.442±0.001	350			
S5-4	100.58	58.13	22.66	19.21	46.2	8.456±0.000	265			
S5-5	100.20	59.46	18.29	22.25	55.3	8.474±0.000	190			
S5-6	100.50	61.45	9.19	29.36	79.2	8.507±0.002	15			

* These samples are contaminated by small amount of SiO_2 which is caused by silica tube.

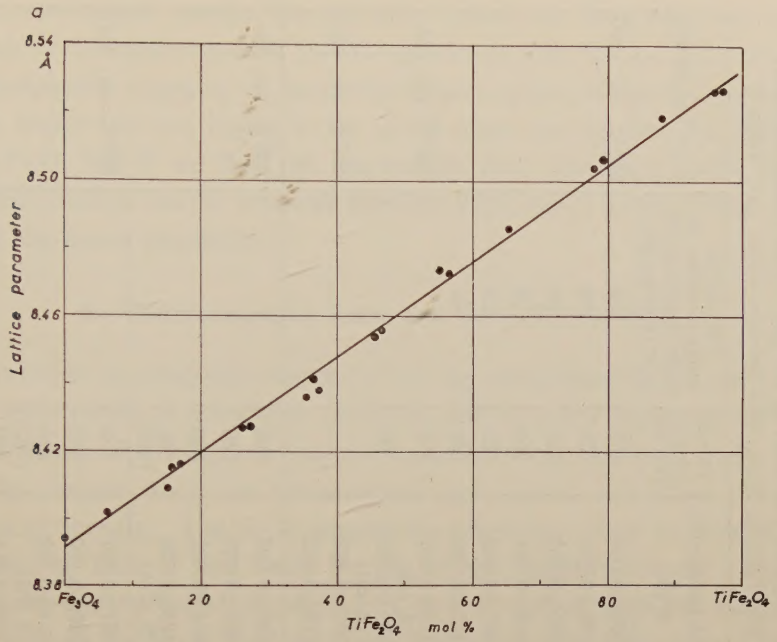

Fig. 2 Relation between lattice parameter and chemical composition in $TiFe_2O_4$–Fe_3O_4 solid solution series.

as a single phase in the region between $TiFe_2O_4$–Fe_3O_4 join and $TiFeO_3$–Fe_2O_3 join. We also obtained the cubic solid solutions in the concerned region by oxidizing the $TiFe_2O_4$–Fe_3O_4 series specimen.

The specimens of $TiFe_2O_4$–Fe_3O_4 solid solution series, packed in an open air porcelain boat, were inserted into an electric furnace after the temperature in the furnace had settled at the designated temperature, and after being maintained there for a designated length of time, taken out and cooled in air. The length of the heat treatment was two hours in most cases and the temperature of heat treatment was the intermediate between 400°C and 550°C.

Ten specimens from S 2–1 to S 2–10 and other four specimens S 5–1, S 5–3, S 5–5 and S 5–6, described in just preceding section, were used for the present purpose. Chemical compositions of the heat-treated specimens are also plotted by hollow circles in Fig. 1 and given in Table II. The heat-treated specimens are distinguished in the figure or table by a mark ′ or ″ from the original ones. As seen in Fig. 1, the chemical composition of the original specimen was shifted by the heat treatment towards the directions of arrows presented in the figure along the theoretical reduction-oxidation line.

The X-ray analysis by the "Norelco" X-ray diffractometer revealed that the specimens still kept their spinel structure after the heat treatment. As for the greater parts of the specimens (S2–3′, S2–5′, S2–6′, S2–7′, S2–8′, S2–9′, S5–1′, S5–3′, S5–5′, S5–6′, S5–1″, S5–3″, S5–5″ and S5–6″) no trace of the ilmenite-hematite series minerals could be detected on the diffraction chart. But as for the specimen S2–1′, fairly large amounts of ilmenite-hematite series minerals were found. The amounts were estimated

Table II *Chemical composition, crystallographic and magnetic properties of the generalized titanomagnetite. The specimens were obtained by oxidizing the* $TiFe_2O_4$–Fe_3O_4 *solid solution series. (cf.* Table I)

Specimen	Chemical composition				Crystal parameter, a (Å)	Curie point, Θ (°C)	Saturation magnetization at room temperature, σ (e.m.u./gr.)	Heat treatment
	$FeO+Fe_2O_3+TiO_2$ wt%	FeO	Fe_2O_3	TiO_2 mol%				
S2-1′	96.86	36.57	59.39	4.04	8.396±0.001	575	59	500°C, air, 2hr.
S2-2′	96.92	40.75	50.15	9.10	8.396±0.001	570	78	,,
S2-3′	100.46	33.81	51.18	15.01	8.396±0.002	565	50	,,
S2-4′	100.01	40.80	40.89	18.31	8.404±0.001	560	58	,,
S2-5′	100.56	40.78	35.60	23.62	8.407±0.002	565	54	,,
S2-6′	99.12	40.77	33.58	25.65	8.417±0.002	560	41	,,
S2-7′	100.69	52.95	19.38	27.66	8.476±0.001 (8.440)	170		420°C, air, 2hr.
S2-8′	100.45	55.18	14.62	30.19	8.489±0.002 (8.454)	80		,,
S2-9′	100.56	58.30	8.89	32.81	8.507±0.003			440°C, air, 2hr.
S2-10′	98.81	52.86	10.43	36.71	8.519±0.002			,,
S5-1′	100.38	46.52	46.21	7.27	8.400±0.002	550		400°C, air, 3hr.
S5-3′	100.22	41.13	41.03	17.84	8.405±0.002	550		,,
S5-5′	100.19	44.87	30.57	24.56	8.414±0.001	540		,,
S5-6′	100.49	43.54	22.74	33.72	8.423±0.002 (8.474)	505 (140)		,,
S5-1″	100.38	41.31	51.18	7.51	8.391±0.001	570		550°C, air, 1hr.
S5-3″	100.20	36.08	45.52	18.40	8.399±0.000	565		,,
S5-5″	100.22	37.17	37.05	25.78	8.414±0.002 (8.358)	540 (585)		,,
S5-6″	100.49	37.71	27.73	34.56	8.424±0.001	530 (585)		,,

from the diffraction chart to be about 30 percent. The specimens S2–2′, S2–4′ and S2–10′ also contained about 10 percent ilmenite-hematite series minerals.

The lattice parameter determined by the X-ray analysis is also listed in Table II, where we can easily find in comparison with Table I that the crystal parameter of all the specimens was decreased considerably by oxidation.

Even though there have been remained some ambiguities with respect to the composition of the spinel phase of the present heat-treated specimens on account of the contamination of a small amount of rhombohedral phase, it may be safely said

from these experimental results that the spinel phase can be in existence as a single phase in fairly broad region between the $TiFe_2O_4$–Fe_3O_4 join and the $TiFeO_3$–Fe_2O_3 join under an appropriate condition of temperature and oxygen pressure. It may be very probable to expect that the region of the spinel phase can be extended more close to the $TiFeO_3$–Fe_2O_3 join if we find the appropriate heat treatment. The fact that a complete solid solution can be prepared between Fe_3O_4 and γ Fe_2O_3 (Hägg; 1935) may also support the above possibility.

4. Thermomagnetic Curve and Curie Temperature

The variation in magnetic moment of all the synthesized spinel specimens as a function of temperature in a constant magnetic field of a few thousands Oersteds was measured by means of a magnetic balance described in the previous paper (Akimoto; 1954). In the present study the measurement was carried out under the evacuated state of about 10^{-3}mmHg. The Curie temperature determined from the thermomagnetic curve is listed in Table I and Table II. As for the specimens of the $TiFe_2O_4$–Fe_3O_4 solid solution series, the Curie temperature is plotted against chemical composition in Fig. 3, where it can be found that the Curie temperature changes almost linearly with composition from 580°C of Fe_3O_4 down to about −150°C of $TiFe_2O_4$.

As for the specimens with lower Curie temperature the measurement of the thermomagnetic curve down to the liquid nitrogen temperature in a field strength of 8450 Oe was practised by the help of Ishikawa at Institute of Science and Technology, Tokyo University. A few examples of the thermomagnetic curve are shown in Fig. 4, where we can see the peculiar mode of thermomagnetic curve like Néel's *P*-type for

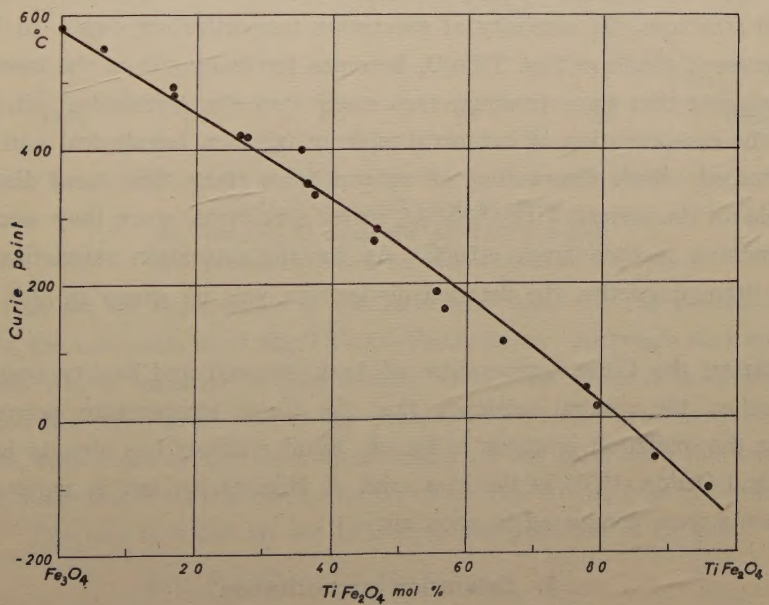

Fig. 3 Relation between Curie temperature and chemical composition in $TiFe_2O_4$–Fe_3O_4 solid solution series.

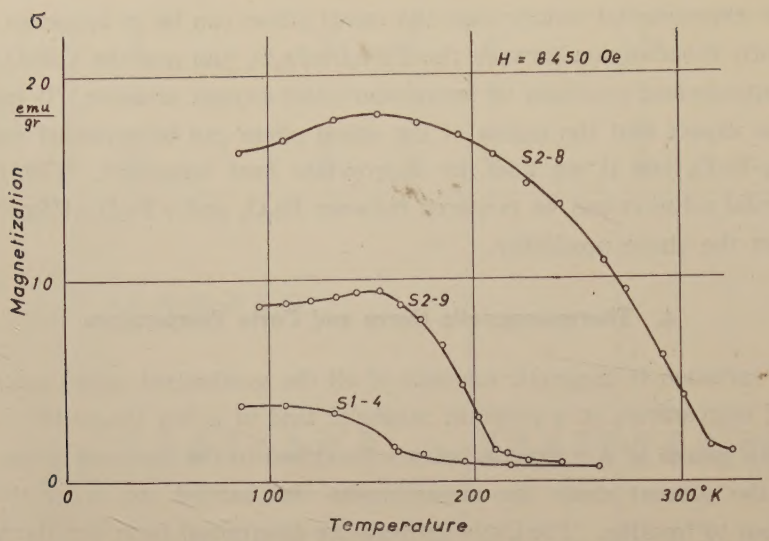

Fig. 4 A few examples of the thermomagnetic curve of $TiFe_2O_4$–Fe_3O_4 solid solution series.

the specimens S2–8 and S2–9. This may be a remarkable contrast to the fact that the thermomagnetic curve of the specimens of which $TiFe_2O_4$ content is less than 60 percent does not show any peculiar mode but is very similar to that of Fe_3O_4. It must be also noticed from Fig. 4 that the specimen of which chemical composition is determined to be $0.96\,TiFe_2O_4 \cdot 0.04\,Fe_3O_4$(S1–4) becomes ferrimagnetic below 170°K, its intensity of magnetization at 80°K in 8450 Oe being about 4 e.m.u./gr. This suggests that pure $TiFe_2O_4$ becomes ferrimagnetic below about 120°K. So long as the inverse spinel structure is kept in $TiFe_2O_4$: that is, titanium ions are confined to the octahedral sites in the spinel structure, the intensity of saturation magnetization ought to be zero at 0°K. The present situation that $TiFe_2O_4$ becomes ferrimagnetic at the lower temperatures may suggest that some titanium ions enter into the tetrahedral sites with the result that the compensation of magnetic moment between tetrahedral and octahedral sites is disturbed. Such disordering of cations from their theoretical distribution is very probable for the present $TiFe_2O_4$–Fe_3O_4 series specimens, since they were prepared by the quenching method from 1150°C. As for the saturation magnetization of the synthesized titanomagnetite, the detailed discussions will be given in the succeeding section.

Comparing the Curie temperature of both original and heat-treated specimens with each other, the general tendency that the Curie temperature becomes higher according as the oxidation proceeds is found. Similar aspect has already been noticed by Nagata and Ozima (1955) in the iron sand of Niisima on which various kinds of heat treatments were conducted in open air.

5. Saturation magnetization

The magnetization curve of the specimen having the higher Curie temperature was measured at the room temperature by means of the magnetic balance up to a

field strength of about 3000 Oe. The intensity of saturation magnetization was determined by extrapolating the following empirical formula to $H=\infty$

$$\sigma=\sigma_s\left(1-\frac{A}{H}\right),$$

where A is the constant determined experimentally for every specimen. As for the specimens with the lower Curie temperature the magnetization curve was measured at the liquid nitrogen temperature by the help of Ishikawa. The intensity of saturation magnetization of the synthesized titanomagnetite at room temperature or 80°K is given in Table I and Table II. The intensity of saturation magnetization of these specimens at 0°K was estimated by extrapolating their thermomagnetic curve to 0°K. These estimated saturation moments of the $TiFe_2O_4$–Fe_3O_4 series specimens are also shown in Table I with the Bohr magneton number per one molecule of $xTiFe_2O_4\cdot(1-x)Fe_3O_4$.

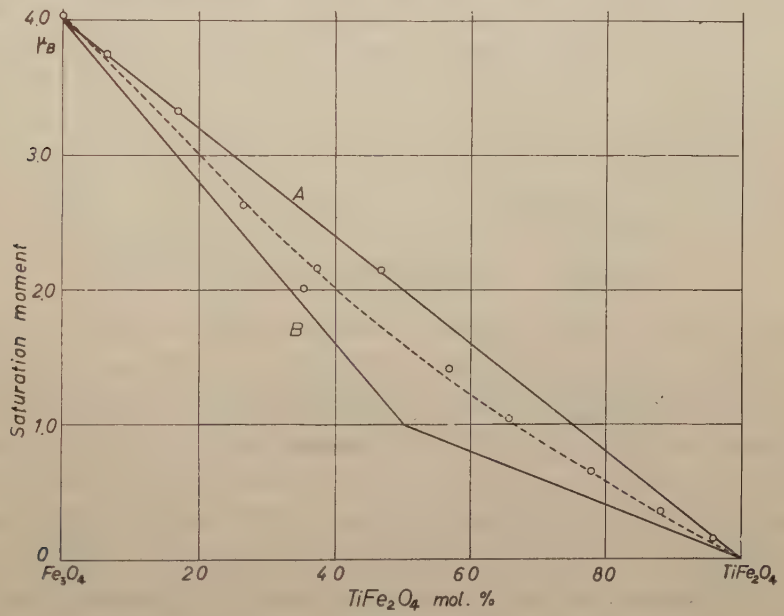

Fig. 5 Estimated saturation moment at 0°K vs. composition for $TiFe_2O_4$–Fe_3O_4 solid solution series.
A: theoretical value for Akimoto's model.
B: theoretical value for Néel-Chevallier's model.

Fig. 5 shows the dependence of the estimated value of the saturation moment at 0°K upon the composition of the $TiFe_2O_4$–Fe_3O_4 series. Although such an estimation as mentioned above includes a considerable error, the general tendency that the magnetization decreases gradually as the content of $TiFe_2O_4$ increases seems to be true. In the figure, two series of the theoretical values on the saturation moment, based on the different assumptions on the configuration of cations in the crystal lattice sites, are also shown. The one is based on the following configuration of cations,

$$Fe^{3+}_{1-x}Fe^{2+}_{x}(Fe^{2+}Fe^{3+}_{1-x}Ti^{4+}_{x})O^{2-}_{4},$$

where the cations inside the bracket indicate the octahedral site and that outside the tetrahedral site of the spinel structure. In this case a saturation moment of $4-4x$ is

calculated (Akimoto; 1954, 1955). The other configuration of cation was postulated by Néel (1955) and Chevallier et al. (1955) by taking the Verwey's empirical law concerning the location of cations in the spinel structure into consideration, that is

$$Fe^{3+}(Fe^{2+}_{1+x}Fe^{3+}_{1-2x}Ti^{4+}_{x})O^{2-}_{4} \qquad \text{for} \quad x<\frac{1}{2}$$

$$Fe^{3+}_{2-2x}Fe^{2+}_{2x-1}(Fe^{2+}_{2-x}Ti^{4+}_{x})O^{2-}_{4} \qquad \text{for} \quad x>\frac{1}{2},$$

for which the saturation moments of $4-6x$ $\left(\text{for } x<\frac{1}{2}\right)$ and $2-2x$ $\left(\text{for } x>\frac{1}{2}\right)$ are calculated.

The actual values of the saturation moments of the synthetic $TiFe_2O_4$–Fe_3O_4 solid solution series are the intermediate between these two. It may also be worthwhile to note that the actual values in our synthetic specimens were always larger than the Néel-Chevallier's theoretical value over the whole range of the composition. This seems to suggest that some titanium ions enter into the tetrahedral sites apart from the normal octahedral sites of $Fe^{3+}(Fe^{2+}_{1+x}Fe^{3+}_{1-2x}Ti^{4+}_{x})O^{2-}_{4}$ or $Fe^{3+}_{2-2x}Fe^{2+}_{2x-1}(Fe^{2+}_{2-x}Ti^{4+}_{x})O^{2-}_{4}$. In these cases, as suggested by Gorter (1957), the cation distribution should be considered as

$$Fe^{3+}_{1-a}Ti^{4+}_{a}(Fe^{2+}_{1+x}Fe^{3+}_{1-2x+a}Ti^{4+}_{x-a})O_4$$

or

$$Fe^{3+}_{2-2x}Fe^{2+}_{2x-1-a}Ti^{4+}_{a}(Fe^{2+}_{2-x+a}Ti^{4+}_{x-a})O_4,$$

the saturation moment being $4-6x+10a$ and $2-2x+8a$ respectively. Then, the saturation moment should be increased with the increase of Ti ions in the tetrahedral sites. As for the present synthetic specimens prepared by the quenching method from high temperature, such disordering of cations may be very probable. Similar effect of the disordering of cations from the ideal inverse spinel structure has already been demonstrated for $MgFe_2O_4$ by Bertaut (1952) and for $NiFeAlO_4$ by Gorter (1954). The implications of such a behaviour for rock magnetism are discussed by Néel (1955) and Verhoogen (1956) in connection with the mechanism causing self-reversal of the remanent magnetization of ferromagnetic minerals. The effect of annealing on the saturation moment of the synthetic specimens is now under investigation.

The variation of saturation moment of the $TiFe_2O_4-Fe_3O_4$ solid solution series with oxidation was also investigated. Comparing the saturation moment of the original specimen (Table I) with the oxidized one (Table II), we may notice the following remarkable situations. That is, the saturation moment at the room temperature of the specimen with the lower content of $TiFe_2O_4$ decreases considerably according as the degree of oxidation proceeds, but that of the specimen with higher content of $TiFe_2O_4$ is increased by oxidation. These experimental results would be explained fairly satisfactorily if we regard the specimen in the intermediate between $TiFe_2O_4$–Fe_3O_4 join and $TiFeO_3$–Fe_2O_3 join as a generalized titanomagnetite having some vacant sites in the structure normally occupied by metallic ions in a spinel and if we assume that the solid solution can be in existence between any composition on the $TiFe_2O_4$–Fe_3O_4 join and the corresponding oxidation product on the $TiFeO_3$–Fe_2O_3 join. It is needless

to say that we must assume here the cubic crystal form on the $TiFeO_3$–Fe_2O_3 join. As for Fe_2O_3, γFe_2O_3 is well known and its magnetic structure is considered to be $Fe^{3+}(Fe^{3+}_{\frac{5}{3}}\square_{\frac{1}{3}})O^{2-}_4$, where $\square$ denotes the vacant site in the structure normally occupied in a spinel. On the other hand as for the cubic form of $TiFeO_3$ magnetic structures of $Fe^{2+}_{\frac{2}{3}}\square_{\frac{1}{3}}(Fe^{2+}_{\frac{2}{3}}Ti^{4+}_{\frac{4}{3}})O^{2-}_4$ and $Fe^{2+}(Ti^{4+}_{\frac{4}{3}}Fe^{2+}_{\frac{1}{3}}\square_{\frac{1}{3}})O^{2-}_4$ have already been postulated by Chevallier et al. (1955) and Nicholls (1955) respectively for interpreting the saturation moment of the $TiFeO_3$–Fe_3O_4 solid solution series. In the present paper hypothetical cubic form of the $TiFeO_3$–Fe_2O_3 system, $y\mathrm{TiFeO_3}\cdot(1-y)\mathrm{Fe_2O_3}$ is taken to be

$$Fe^{3+}_{1-y}Fe^{2+}_{\frac{2}{3}y}\square_{\frac{1}{3}y}(Fe^{3+}_{\frac{5}{3}(1-y)}Fe^{2+}_{\frac{2}{3}y}Ti^{4+}_{\frac{4}{3}y}\square_{\frac{1}{3}(1-y)})O^{2-}_4$$

in making use of the Chevallier's $\gamma TiFeO_3$. This implies that the saturation moment of the cubic $TiFeO_3$–Fe_2O_3 system changes linearly with the composition according to equation

$$M=\frac{10}{3}(1-y)\mu_B.$$

We showed the variation of saturation moment along the reduction-oxidation line in Table III, where the original value of saturation moment of $TiFe_2O_4$–Fe_3O_4 join and the final value of $TiFeO_3$–Fe_2O_3 join are given for different values of Fe/Fe+Ti in the unit of Bohr magneton number per molecule. As for the saturation moment of

Table III *Change in saturation moment of $TiFe_2O_4$–Fe_3O_4 solid solution series with oxidation.*

Fe/Fe+Ti	Original spinel, $x\mathrm{TiFe_2O_4}\cdot(1-x)\mathrm{Fe_3O_4}$			Oxidation product, $y\mathrm{TiFeO_3}\cdot(1-y)\mathrm{Fe_2O_3}$	
	x	saturation moment(μ_B)		y	saturation moment(μ_B)
1.000	0	4.0*		0	3.33
0.966	0.1	3.4	(3.6)**	0.067	3.11
0.933	0.2	2.8	(3.2)	0.133	2.89
0.900	0.3	2.2	(2.8)	0.200	2.67
0.866	0.4	1.6	(2.4)	0.267	2.44
0.833	0.5	1.0	(2.0)	0.333	2.22
0.800	0.6	0.8	(1.6)	0.400	2.00
0.766	0.7	0.6	(1.2)	0.467	1.78
0.733	0.8	0.4	(0.8)	0.533	1.56
0.700	0.9	0.2	(0.4)	0.600	1.33
0.666	1.0	0		0.667	1.11

* after Néel-Chevallier's model.
** after Akimoto's model.

$TiFe_2O_4$–Fe_3O_4 join, two sets of values are listed in the table; i.e. Néel-Chevallier's value (Néel; 1955, Chevallier et al.; 1955) and the value postulated previously by one of the authors (Akimoto; 1954). From the table it is clearly seen that the saturation moment of the specimen with lower content of $TiFe_2O_4$ decreases according as the oxidation proceeds, while that of the higher content of $TiFe_2O_4$ increases. This situation accords well at least qualitatively with the above-mentioned experimental results.

6. Conclusive Remarks

The accumulation of the reliable data on the chemical, crystallographic and magnetic properties of the spinel specimens enables us to draw an equal lattice constant line, equal Curie point line or equal saturation moment line on the spinel region in the

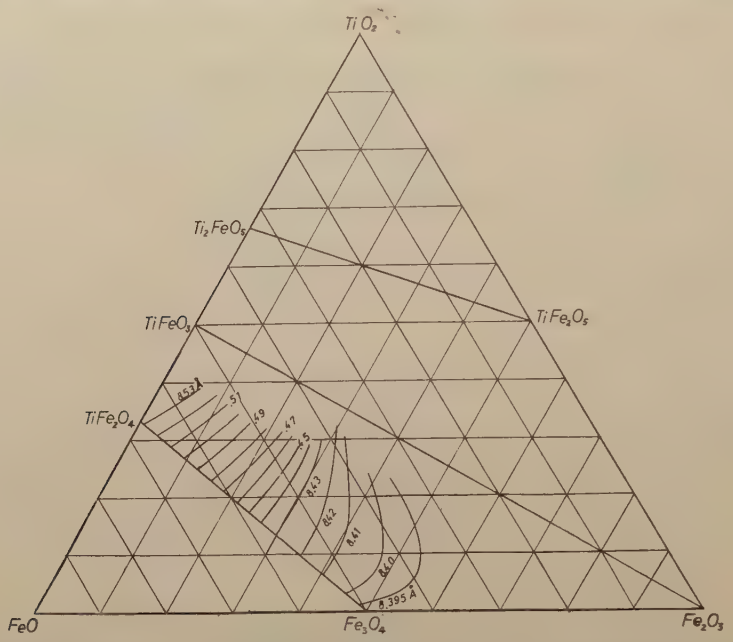

Fig. 6 Lines of equal lattice parameter of the generalized titanomagnetite in a FeO–Fe_2O_3–TiO_2 system.

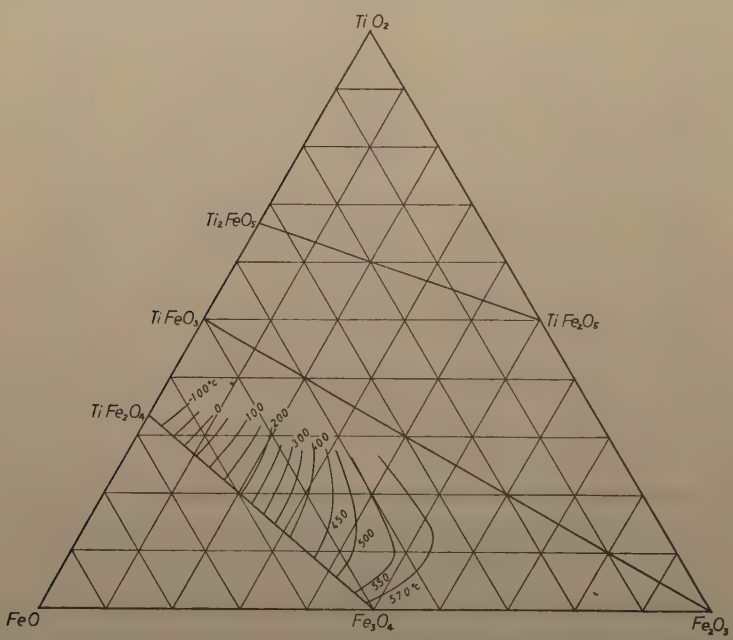

Fig. 7 Lines of equal Curie temperature of the generalized titanomagnetite in a FeO–Fe_2O_3–TiO_2 system.

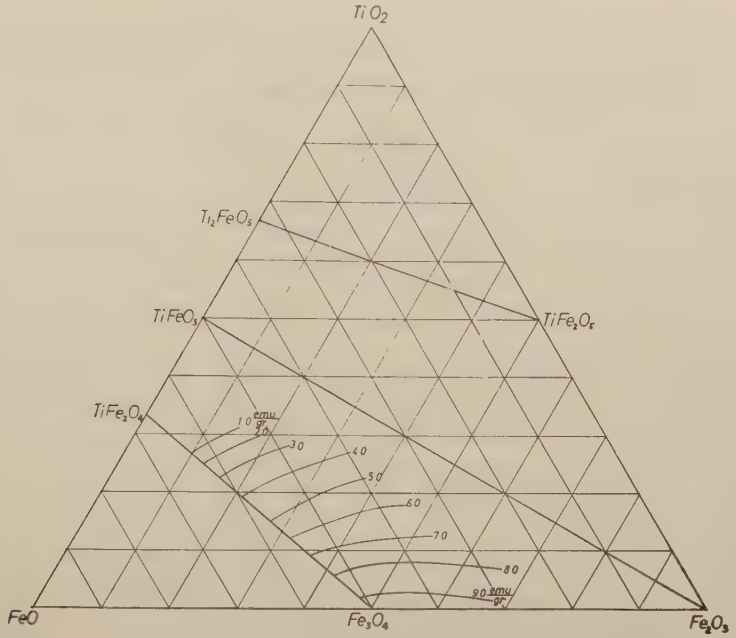

Fig. 8 Lines of equal saturation moment at the room temperature of the generalized titanomagnetite in a FeO–Fe_2O_3–TiO_2 system.

FeO–Fe_2O_3–TiO_2 system. Figs. 6, 7 and 8 are the equal lattice parameter diagram, equal Curie point diagram and equal saturation moment diagram respectively. The results of Chevallier and Girard's study (1950) are also taken into account in drawing these diagrams.

It can be easily found from these diagrams that the general view of the equal lattice parameter diagram and the equal Curie point diagram resembles very much with each other; that is, the parallelism of the equal lattice parameter line and the equal Curie point line is generally found. Another remarkable character found in these diagrams is that the equal Curie point line representing the temperature higher than about 500°C has a marked curvature in contrast to the straight line of the lower temperatures.

It must also be mentioned here that such an attempt to draw an equal Curie point line on the FeO–Fe_2O_3–TiO_2 system has already been done by Chevallier and Girard (1950). They suggested the Curie point variation may be expressed by

$$\theta°\mathrm{K}\ (\text{Curie point}) = 1245s$$

where

$$s = \frac{\mathrm{wt}\%\mathrm{Fe_2O_3}}{\mathrm{wt}\%\mathrm{Fe_2O_3} + \mathrm{FeO}} \ .$$

The present diagram shown in Fig. 7 accords well with that postulated by them within the Fe_3O_4–$TiFeO_3$–$TiFe_2O_4$ system except higher temperature side.

The general view of the equal saturation moment diagram differs greatly from other two diagrams, that is, the equal saturation moment line intersects the equal lattice parameter line or the equal Curie point line in the FeO–Fe_2O_3–TiO_2 diagram.

These diagrams seem to have a deep significance especially in the field of

geological application of rock magnetism. It has already been shown that the magnetic analysis, together with chemical and X-ray analyses, is sometimes useful for determining the constitution of the ferromagnetic minerals contained in rocks. As the present diagrams show, however, the chemical composition having a definite lattice parameter or Curie point is not represented by a point but form a line on the FeO–Fe_2O_3–TiO_2 system. Hence, even if the lattice parameter or Curie point of the ferromagnetic minerals were determined with sufficient accuracy by X-ray or magnetic analysis, it is impossible to fix their chemical composition to a point on the FeO–Fe_2O_3–TiO_2 system. The determination of the chemical composition by these method is always accompanied with some uncertainties. When we measure the saturation moment of the specimen at the same time, this uncertainty will vanish, the chemical composition of the specimen being able to be fixed to a single point. It is also expected that the reliable data on the specific gravity of the specimen is useful for the determination of the chemical compositions.

In concluding the present paper, the authors wish to express their sincere thanks to Prof. T. Nagata for his constant guidance throughout the study. They also wish to thank Prof. I. Iwasaki for his kind encouragement and interest. The authors are also indebted to Dr. Y. Ishikawa for his magnetic measurement at lower temperatures.

References

Akimoto. S., 1954, Journ. Geomag. Geoelect., **6**, 1.
1955, Jap. Journ. Geophysics, **1**, No. 2, 1.
Bertaut, F., 1952, C. R. Acad. Sci. Paris, **234**, 1295.
Chevallier, R., and Girard, J., 1950, Bull. Soc. Chem. France, **5**, **17**, 576.
Chevallier, R., Bolfa, J. and Mathieu, S., 1955, Bull. Soc. Franc. Miner. Crist., **78**, 307, 365.
Ernst, T., 1943, Zeits. angew. Min., **4**, 394.
Gorter, E.W., 1954, Philips Res. Rep., **9**, 295, 321, 403.
1957, Advanc. Phys., **6**, 336.
Hägg, G., 1935, Zeits. Phys. Chem., **29**, 95.
Kawai, N., Kume, S., and Sasajima, S., 1954, Proc. Japan Acad., **30**, 588.
Nagata, T. and Ozima, M., 1955, Journ. Geomag. Geoelect., **7**, 105.
Néel, L., 1955, Advanc. Phys., **4**, 191.
Nicholls, G.D., 1955, Advanc. Phys. **4**, 113.
Pouillard, E., 1950, Ann. Chimie, **5**, 164.
Verhoogen, J., 1956, Journ. Geophys. Res., **61**, 201.

The Variation Type of the Atmospheric Potential Gradient and the Geographic latitude of the Globe

By Miyoji GOTO

Aso Institute, Kyoto University

(Read May 16, 1953; Received March 20, 1958)

The global distribution of the annual and diurnal variation of the atmospheric potential gradient is discussed, using the material which is derived from H. Benndorf (1928) as shown in Table 1. Making use of A (Jahresamplitude des P.G. in V/m) and

Table 1

Laufende Nr.	Beobachtungsort	Geogr. Breite	Beobachtungszeit	Jahresmittel des P.G. in V/m	Jahresamplitude des P.G. in V/m(A)	Tagesamplitude des P.G. in V/m(D)	A/D
1	Ebeltofthafen	79.1°N	1913–1914	95	76	16	4.75
2	Karasjok	69.3°N	1903–1904	139	119	110	1.08
3	Vassijaure	68.4°N	1909–1910	89	110	50	2.2
4	Upsala	59.9°N	1912–1914	70	59	50	1.18
5	Aas	59.7°N	1916–1923	104	105	46	2.28
6	Eskdalemuir	55.3°N	1914–1920	263	161	109	1.47
7	Potsdam	52.4°N	1904–1923	202	127	72	1.76
8	Kew	51.5°N	1898–1920	317	239	130	1.83
9	Val Joyeux	48.8°N	1923–1924	90	63	48	1.31
10	München	48.1°N	1905–1910	168	161	132	1.22
11	Kremsmünster	48.1°N	1902–1916	105	79	60	1.32
12	Davos	46.8°N	1908–1910	64	68	44	1.54
13	Triest	45.6°N	1902–1905	73	25	86	0.29
14	Tortosa	40.8°N	1910–1924	106	37	57	0.65
15	Washington	39.0°N	1920–1923	179	—	—	—
16	Helwan	29.8°N	1909–1914	150	54	61	0.88
17	Batavia	6.2°S	1890–1900	120	53	145	0.36
18	Apia	13.8°S	1913–1924	112	22	92	0.24
19	Rio de Janeiro	22.9°S	1910–1914	128	80	—	—
20	Buenos Aires	34.5°S	1911–1912	136	78	101	0.77
21	Melbourne	37.8°S	1858–1860	145	75	125	0.60
22	Petermannsinsel	65.2°S	1909	164	190	92	2.06
23	Cap Evans	77.6°S	1911–1912	87	40	30	1.33
24	Mc Murdo Sund	77.8°S	1902–1903	93	63	—	—
25	Auf dem Ozean (Carnegie fahrt)	80°N 60°S	1915–1921	124	20	43	0.46

D (Tagesamplitude des P.G. in V/m) from the Table, the ratio A/D for each stations can be calculated numerically as indicated beside the Table 1. Then the whole stations on the globe can be divided into two groups according to $A/D>1$ and $A/D<1$.

The relation between the ratio A/D and geographic latitude of each stations is shown graphically in Fig. 1. From Fig. 1 we can see distinctly that the stations in which $A/D>1$ are all located in the high latitude regions, northwards from 46°N and southwards from 46°S in both hemisphers, and the remaining stations in which $A/D<1$ are all located in the low latitude zone from 46°N to 46°S. Judging from $A/D=0.46<1$ from the data of the Carnegie cruise on the ocean from 80°N to 60°S, it is thought that these data may be mainly from the wide sea area of the low latitude zone. As above mentioned, the high latitude caps and low latitude belt can be distinguished distinctly with respect to the annual and diurnal variations of the atmospheric potential gradient. It is desirable to make an observation in the neighbourhood of the transitional latitude (46°) in both hemispheres, especially in southern hemisphere.

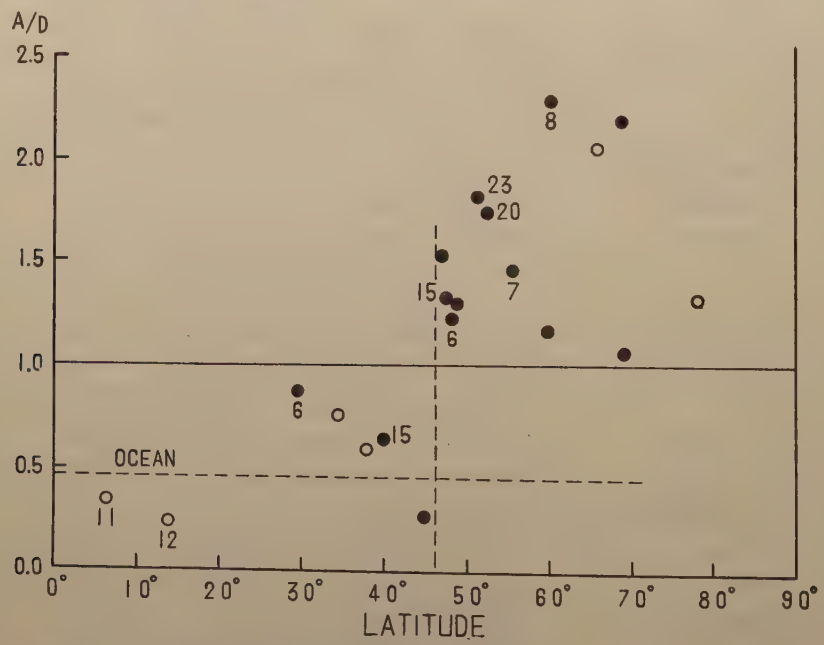

Fig. 1 ● Station in northern hemisphere.
○ Station in southern hemisphere.
Figure aside the point means the number of observation to be available.
Point without figure indicates that the period of observation is less than five years.

With regard to the feature of the mode of the annual variation of potential gradient H. Benndorf has divided the whole stations into two groups, A and B, geographically.

A group stations, northwards from 30°N and southwards from 40°S (Nord-und Südpolarkappen) indicate the marked einfachen jährlichen Gang, maximum in winter solstice and minimum in summer solstice, and B group stations, from 30°N to 40°S

(Äquatorialgürtel) indicate somewhat different mode of annual variation, maximum in Juli-Aug and minimum in Nov-März.

It is supposed that the mode of the annual variation of the potential gradient suggested by H. Benndorf and the global distribution of the ratio A/D have deep mutual connection each other. It is too hasty to state the unique interpretation governing the above mentioned world wide phenomena, but we may say in moderation that judging from $A/D>1$, the high latitude caps predominate the world wide annual variation, and from $A/D<1$, the low latitude belt predominates the world wide diurnal variation.

From the above consideration it may be said that the upper conducting layer is not unique as hitherto considered, but somewhat complicated in structure.

This paper was read at the meeting of the Society of Terrestrial Magnetism and Electricity of Japan held at Tokyo on May 1953. The writer wishes to express his thanks to Dr. Prof. Y. Tamura and Dr. H. Hatakeyama for their helpful encouragement.

Reference

Benndorf, H.: Atmosphärische Elektrizität. Handbuch der exp Phys. Bd. 25. Geophys. 1. Teil. (1928)

Fluid Motions in a Sphere I

Thermal Instability of a Rotating Fluid Sphere Heated within

By Tomikazu NAMIKAWA

Institute of Politechnics, Osaka City University

(Read Oct. 9, 1957; Received July 20, 1958)

Abstract

Thermal instability of an incopressible rotating fluid sphere with negligible viscosity heated within is examined. It is found that we are not able to have stationary convections; Instability first sets in as overstability.

I. Introduction

In recent years the onset of thermal instability in horizontal layers of viscous fluid, heated from below under the influence of Coriolis acceleration and magnetic field has been investigated [1]–[4]. These studies have disclosed a number of novel features. Extent of these investigation to a fluid sphere was carried out by Chandrasekhar [5] and to a rotating sphere by Takeuchi and Shimazu [6] and Chandrasekhar [7] in the case of axial symmetry under modified boundary conditions. We are interested in the convection in the earth's core or in the stars under the influence of Coriolis force and magnetic field. The present paper is devoted, as the first step, to problems of a rotating fluid sphere with internal heat sources.

2. The Equation of the Problem

We shall consider a homogeneous sphere of radious a rotating with an angular velocity Ω about the z-axis. A heat generating source is supposed. The rate of heat generation is assumed such that in the absence of conduction and convection the temaerature would rise at a uniform rate ε. The deduction of the equation governing small departures was done by Chandrasekhar [5], [7]. The treatment is given in appendix.

The temperature ditributions in the state of no convection is given by

$$T=\beta(a^2-r^2), \quad \beta=\varepsilon/6\kappa, \tag{1}$$

where κ is the coefficient of thermometric conductivity. The equations governing small departures from the stationary state are [A, (14), (15)]

$$\frac{\partial\theta}{\partial t}=\kappa\nabla^2\theta+2\beta(ru_r), \tag{2}$$

$$\frac{\partial \boldsymbol{u}}{\partial t}=-\nabla\frac{\delta p}{\rho_0}+\gamma\theta\boldsymbol{r}+\nu\nabla^2\boldsymbol{u}+2\boldsymbol{u}\times\boldsymbol{\Omega}, \tag{3}$$

and

$$\operatorname{div}\boldsymbol{u}=0, \tag{4}$$

where θ is the perturbations in temperature.

We can elminate δp from eqn. (3). by taking its curl. Making use of eqn. (4). we have

$$\frac{\partial \boldsymbol{\omega}}{\partial t}=\gamma \nabla\theta\times\boldsymbol{r}+\nu\nabla^2\boldsymbol{\omega}+2\Omega\frac{\partial \boldsymbol{u}}{\partial z}, \tag{5}$$

where $\boldsymbol{w}$ denotes the vorticity. Next, by taking the curl of eqn. (5), we obtain

$$-\frac{\partial}{\partial t}\nabla^2\boldsymbol{u}=\gamma\,\mathrm{curl}(\nabla\theta\times\boldsymbol{r})-\nu\nabla^4\boldsymbol{u}+2\Omega\frac{\partial \boldsymbol{\omega}}{\partial z}\ . \tag{6}$$

We can express the velocity field as a superposition of poloidal and toroidal vector in terms of two scalars.

$$\boldsymbol{u}=\nabla T\times\boldsymbol{i}_r+\mathrm{curl}(\nabla S\times\boldsymbol{i}_r), \tag{7}$$

where $\boldsymbol{i}_r$ is the unit vector of radious direction. Two scalars T and S are expressed as follows

$$T=\sum_{m,n}T_n^m(r,\ t)Y_n^m \text{ and } S=\sum_{m,n}S_n^m(r,\ t)Y_n^m\ , \tag{8}$$

where Y_n^m is a surface spherical harmonic.

The following procedure is equivalent to take the poloidal and the toroidal components of eqn. (5).

Multiplying eqn. (5) by $\boldsymbol{r}$, we get

$$\frac{\partial(r\omega_r)}{\partial t}=\nu\nabla^2(r\omega_r)+2\Omega\boldsymbol{r}\frac{\partial \boldsymbol{u}}{\partial z}, \tag{9}$$

and

$$-\frac{\partial}{\partial t}\nabla^2(rur)=\gamma L^2\theta-\nu\nabla^4(ru_r)+2\Omega\boldsymbol{r}\frac{\partial \boldsymbol{\omega}}{\partial z}, \tag{10}$$

where

$$L^2=r^2\left(\frac{\partial^2}{\partial r^2}+\frac{r}{2}\frac{\partial}{\partial r}-\nabla^2\right).$$

We express $\theta=\sum_{m,n}\Theta_n^m(r,\ t)Y_n^m$. Operating Y_n^m to eqns. (2), (9) and (10) and executing the integration with respect to ϑ and φ, we get

$$\frac{\partial}{\partial t}\Theta_n^m-\kappa\frac{1}{r^2}\left\{\frac{d}{dr}\left(r^2\frac{d}{dr}\right)-n(n+1)\right\}\Theta_n^m-2\beta n(n+1)\frac{S_n^m}{r}=0, \tag{11}$$

$$\frac{\partial}{\partial t}n(n+1)\frac{T_n^m}{r}-\nu n(n+1)\frac{1}{r^2}\left\{\frac{d}{dr}\left(r^2\frac{d}{dr}\right)-n(n+1)\right\}\frac{T_n^m}{r}-2\Omega\left\{\frac{(n-1)(n+1)(n-m)}{2n-1}\right.$$
$$\left.\times r^{n-1}\frac{d}{dr}(r^{-n}S_{n-1}^m)+\frac{n(n+2)(n+m+1)}{2n+3}r^{-(n+2)}\frac{d}{dr}(r^{n+1}S_{n+1}^m)+im\frac{T_n^m}{r}\right\}=0, \tag{12}$$

and

$$-n(n+1)\frac{\partial}{\partial t}\frac{1}{r^2}\left\{\frac{d}{dr}\left(r^2\frac{d}{dr}\right)-n(n+1)\right\}\left\{\frac{S_n^m}{r}+\nu n(n+1)\left[\frac{1}{r^2}\left\{\frac{d}{dr}\left(r^2\frac{d}{dr}\right)\right.\right.\right.$$
$$\left.\left.\left.-n(n+1)\right\}\right]^2\frac{S_n^m}{r}-2\Omega\left[\frac{(n-1)(n+1)(n-m)}{2n-1}r^{n-1}\frac{d}{dr}(r^{-n}T_{n-1}^m)\right.\right.$$
$$\left.\left.+\frac{n(n+2)(n+m+1)}{2n+3}r^{-(n+2)}\frac{d}{dr}(r^{n+1}T_{n+1}^m)-im\frac{1}{r}\left\{\frac{d^2}{dr^2}-\frac{n(n+1)}{r^2}\right\}S_n^m\right]\right.$$
$$=\gamma n(n+1)\Theta_n^m. \tag{13}$$

The following transformation of notations are made

$$r'=\frac{r}{a} \quad \text{and} \quad T_n^m(r,\ t)=\frac{1}{r}T'^m_n(r,\ t), \tag{14}$$

but for simplicity, we write r' and $T_n^m(r,\ t)$ as r and $T_n^m(r,\ t)$. Thus eqns. (11), (12) and (13) becomes as follows.

$$\frac{\partial}{\partial t}a^2\Theta_n^m-\kappa\frac{1}{r^2}\left\{\frac{d}{dr}\left(r^2\frac{d}{dr}\right)-n(n+1)\right\}\Theta_n^m-2\beta an(n+1)\frac{S_n^m}{r}=0, \tag{15}$$

$$n(n+1)a^2\frac{\partial}{\partial t}\frac{T_n^m}{r^2}-\nu n(n+1)\frac{1}{r^2}\left\{\frac{d}{dr}\left(r^2\frac{d}{dr}\right)-n(n+1)\right\}\frac{T_n^m}{r^2}$$
$$-2\Omega a^2\left\{\frac{(n-1)(n+1)(n-m)}{2n-1}r^{n-1}\frac{d}{dr}(r^{-n}S_{n-1}^m)+\frac{n(n+2)(n+m+1)}{2n+3}\right.$$
$$\left.\times r^{-(n+2)}\frac{d}{dr}(r^{n+1}S_{n+1}^m)+im\frac{T_n^m}{r^2}\right\}=0, \tag{16}$$

and

$$-n(n+1)a^2\frac{\partial}{\partial t}\frac{1}{r^2}\left\{\frac{d}{dr}\left(r^2\frac{d}{dr}\right)-n(n+1)\right\}\frac{S_n^m}{r}+\nu n(n+1)\left[\frac{1}{r^2}\left\{\frac{d}{dr}\left(r^2\frac{d}{dr}\right)\right.\right.$$
$$\left.\left.-n(n+1)\right\}\right]^2\frac{S_n^m}{r}-2\Omega a^2\left[\frac{(n-1)(n+1)(n-m)}{2n-1}r^{n-1}\frac{d}{dr}(r^{-n-1}T_{n-1}^m)\right.$$
$$+\frac{n(n+2)(n+m+1)}{2n+3}r^{-(n+2)}\frac{d}{dr}(r^nT_{n+1}^m)-im\frac{1}{r}\left\{\frac{d^2}{dr^2}-\frac{n(n+1)}{r^2}\right\}S_n^m\Big]$$
$$=\gamma n(n+1)a^5\Theta_n^m \tag{17}$$

Equations (15), (16) and(17) are the basic equations of this problem.

3. Boundary Conditions

We treat eqns. (15), (16) and (17) neglecting the viscous term. This simplification is allowed when we consider some geophysical or astrophysical problems. For example, in the Earth's Core, kinematic viscosity is estimated to be $10^{-3}\sim10^{9}$. The order of magnitude of viscous force, $\rho_0\nu U/a^2$, is $10^{-20}\sim10^{-8}$, which is much smaller than 10^{-4}, order of magnitude of Coriolis force [9].

Thus boundary conditions are not dependent on whether the bounding surface considered is rigid or free. In all cases, we require that

$$\theta=0 \quad \text{and} \quad u_r=0 \qquad \text{(on a bounding spherical surface)} \tag{18}$$

4. The Solutions of Basic Equations

From eqns. (15), (16) and (17), we can find that there exist groups of fluid motions which contain S_n^m or T_n^m with $n=m$ as their first number. Axially symmetric case is an exceptional one from this rule.

The way of coupling of fluid motions is shown schematically as follows

$$S_1^0 \rightleftarrows T_2^0 \rightleftarrows S_3^0 \quad \cdots\cdots$$
$$T_1^0 \rightleftarrows S_2^0 \rightleftarrows T_3^0 \quad \cdots\cdots$$
$$S_1^1 \rightleftarrows T_2^1 \rightleftarrows S_3^1 \quad \cdots\cdots$$
$$T_1^1 \rightleftarrows S_2^1 \rightleftarrows T_3^1 \quad \cdots\cdots$$
$$S_2^2 \rightleftarrows T_3^2 \rightleftarrows S_4^2 \quad \cdots\cdots$$

$$T_2^2 \rightleftarrows S_3^2 \rightleftarrows T_4^2 \quad \cdots\cdots \tag{18}$$

$$\cdots\cdots\cdots\cdots\cdots$$

etc.

We can satisfy the boundary conditions on $\Theta_n^m(r, t)$ and $S_n^m(r, t)$ by expanding them in terms of the various modes which form a complete set of orthogonal functions. Thus

$$\Theta_n^m(r, t)=\sum_j \Theta_{n,j}^m \frac{J_{n+\frac{1}{2}}(\alpha_j r)}{\sqrt{r}} \quad \text{and} \quad \frac{S_n^m(r, t)}{r}=\sum_j S_{n,j}^m \frac{J_{n+\frac{1}{2}}(\alpha_j r)}{\sqrt{r}}, \tag{18}$$

where $J_{n+\frac{1}{2}}$ demote the Bessel functions of order $n+1/2$. The α_j's ($j=1, 2, \ldots.$) are its zeros.

5. An Examination of the Principle of the Exchagne of Stabilities

a) $[S_n^m, T_{n+1}^m, \ldots.]$ motion

We shall first examine stability of $[S_n^m, T_{n+1}^m, \ldots.]$ motion taking only the first two motions S_n^m and T_{n+1}^m. It seems that this simplification does not alter the results to any great extent [6], [7]. We expand $S_n^m(r, t)$, $T_{n+1}^m(r, t)$ and $\Theta_n^m(r, t)$ as follows,

$$\frac{S_n^m(r, t)}{r}=\sum_j S_{n,j}^m \frac{J_{n+\frac{1}{2}}(\alpha_j r)}{\sqrt{r}}, \quad \frac{T_n^m}{r^2}=\sum_j T_{n+1,j}^m \frac{J_{n+\frac{3}{2}}(\alpha_j r)}{\sqrt{r}}$$

and

$$\Theta_n^m(r, t)=\sum_j \Theta_{n,j}^m \frac{J_{n+\frac{1}{2}}(\alpha_j r)}{\sqrt{r}}, \tag{20}$$

where α_j's are the jth roots of $J_{n+\frac{1}{2}}(\alpha_j)=0$.

If all quantities very like $e^{\lambda t}$, eqns. (15), (16) and (17) are reduced to

$$(\lambda a^2+\kappa\alpha_j^2)\Theta_{n,j}^m-2\beta a n(n+1)S_{n,j}^m=0, \tag{21}$$

$$(n+1)(n+2)\lambda a^2 T_{n+1,j}^m-2\Omega a^2\left\{-\frac{n(n+2)(n+1-m)}{2n+1}\alpha_j S_{n,j}^m+imT_{n+1,j}^m\right\}=0 \tag{22}$$

and

$$n(n+1)\lambda a^2\alpha_j^2 S_{n,j}^m-2\Omega a^2\left\{\frac{n(n+2)(n+m+1)}{2n+3}\alpha_j T_{n+1,j}^m+im\alpha_j^2 S_{n,j}^m\right\}$$
$$-\gamma n(u+1)a^5\Theta_{n,j}^m=0. \tag{23}$$

From above equations we get

$$\{(n+1)(n+2)\omega-im\kappa T\}\left\{n(n+1)\alpha_j^2\omega-im\alpha_j^2\kappa T-\kappa^2\frac{n^2(n+1)^2}{\omega+\kappa\alpha_j^2}R\right\}$$
$$+\frac{n^2(n+2)^2(n+m+1)(n+1-m)}{(2n+1)(2n+3)}\alpha_j^2\kappa^2T^2=0, \tag{24}$$

where

$$\omega=\lambda a^2, \quad T=\frac{2\Omega}{\kappa}a^2 \quad \text{and} \quad R=\frac{2\beta\gamma}{\kappa^2}a^6. \tag{25}$$

Eqn. (24) is reduced to

$$\omega^3+(p_1+ip_2)\omega^2+(q_1-R_1+ip_1p_2)\omega+p_1q_1+i\frac{m\kappa T}{(n+1)(n+2)}R_1=0, \tag{26}$$

where

$$\left.\begin{aligned} &p_1=\kappa\alpha_j{}^2, \qquad p_2=-2m\kappa T, \\ &q_1=\left\{\frac{n(n+2)(n+m+1)(n+1-m)}{(n+1)^2(2n+1)(2n+3)}-\frac{m^2}{n(n+1)^2(n+2)}\right\}\kappa^2T^2 \text{ and } R_1=\frac{n(n+1)}{\alpha_j{}^2}\kappa^2R. \end{aligned}\right\} \tag{27}$$

Substituting $\omega=x+iy$ in eqn. (26), we get

$$x^3+p_1x^2-(3_1y^2+2p_2y-q_1+R_1)x-p_1y^2-p_1p_2y+p_1p_1=0 \tag{28}$$

and

$$(3y+p_2)x^2+p_1(2y+p_2)x-y^3-p_2y^2+(q_1-R_1)y+\frac{m\kappa T}{(n+1)(n+2)}R_1=0. \tag{29}$$

As p_1, q_1 and $\frac{m\kappa T}{(n+1)(n+2)}$ are positive, we have no steady state solutions.

i) axially symmetric solutions

In this case, eqn. (26) is reduced to

$$\omega^3+p_1\omega^2+(q_1-R_1)\omega+p_1q_1=0 \tag{30}$$

When $q_1-R_1<0$ this eqn. is able to have positive real roots, but when $q_1-R_1>0$ it is not possible to have positive real roots. Eqn. (30) allows a negative real root and the corresponding solutions lead to an exponential damping of an initial disturbance. We have to examine whether under these conditions the complex roots of (30) can have a positive real part. If x and y denote the real and the imaginary parts of complex roots of eqn. (30), they must satisfy the equations

$$3x^2+2p_1x+q_1-R_1=y^2 \tag{31}$$

and

$$x^3+p_1x^2+(q_1-R_1)x+p_1q_1-(3x+p_1)y^2=0. \tag{32}$$

From the above two eqns. we have

$$8x^3+8p_1x^2+2(p_1^2+q_1-R_1)x-p_1R_1=0. \tag{33}$$

This eqn. admits a positive real root and letting $R_1\to0$, we shall have the critical frevuency

$$\lambda=\frac{\kappa T}{\sqrt{5}\,a^2}=\frac{2\Omega}{\sqrt{5}}. \tag{34}$$

Thus we know the critical frequency of axially symmetric oscillation of a rotating non viscus fluid sphere is nearly equal to the angular velocity of the sphere.

ii) asymmetric solutions

The real roots of eqn. (26) must satisfy the equations

$$x^3+p_1x^2+(q_1-R_1)x+p_1q_1=0 \tag{35}$$

and

$$p_2x^2+p_1p_2x+\frac{m\kappa T}{(n+1)(n+2)}R_1=0 \tag{36}$$

As $p_2<0$ and the third term of eqn. (36) is positive, eqn. (36) has a positive and a negative real roots. When $q_1-R_1<0$, eqn. (35) is able to have a positive root, but when $q_1-R_1>0$ this has a negtive root.

From eqns. (35) and (36) we get

$$x=\frac{-p_1q_1}{q_1-\dfrac{2(n+1)(n+2)-1}{2(n+1)(n+2)}R_1}. \tag{37}$$

When

$$R_1>\frac{2(n+1)(n+2)}{2(n+1)(n+2)-1}q_1>q_1\,, \tag{38}$$

we have postive value of x.

When eqn. (26) has no positive roots, its complex roots must satisfy

$$x^3+p_1x^2-\{(y^2+p_2y-q_1)+y(2y+p_2)+R_1\}x-p_1(y^2+p_2y-q_1)=0 \tag{39}$$

and

$$(3y+p_2)x^2+p_1(2y+p_2)x-y(y^2+p_2y-q_1)+R_1\left\{\frac{m\kappa T}{(n+1)(n+2)}-y\right\}=0. \tag{40}$$

Eqn. (39) admits positive roots when

$$y^2+p_2y-q_1>0 \tag{41}$$

Eqn. (40) admits a positive root when

$$3y+p_2>0, \tag{42}$$

and

$$-y(y^2+p_2y-q_1)+R_1\left\{\frac{m\kappa T}{(n+1)(n+2)}-y\right\}<0. \tag{43}$$

General examination of the inequality of(41), (42) and (43) is troublesome, but these inequality can be clearly satisfied by the condition

$$y>\frac{m\kappa T}{(n+1)(n+2)} \tag{44}$$

Thus we have a case of overstability when period of oscillation is smaller than a critical value. The critical number of vibrations is

$$\lambda=\frac{2m}{(n+1)(n+2)}\Omega \tag{45}$$

which is smaller than the angular velocity of sphere for all value of n tends to zero when n tends to infinity.

b) $[T_n^m,\ S_{n+1}^m,\ \cdots\cdots]$ motion

We express $T_n^m(r,\ t)$, $S_{n+1}^m(r,\ t)$ and $\Theta_{n+1}^m(r,\ t)$ as follows

$$\frac{T_n^m(r,t)}{r^2}=\sum_j T_{n,j}^m\frac{J_{n+\frac{1}{2}}(\alpha_j r)}{\sqrt{r}},\quad \frac{S_{n+1}^m(r,t)}{r}=\sum_j S_{n+1,j}^m\frac{J_{n+\frac{1}{2}}(\alpha_j r)}{\sqrt{r}} \tag{46}$$

and

$$\Theta_{n+1}^m(r,\ t)=\sum_j\Theta_{n+1,j}^m\frac{J_{n+\frac{1}{2}}(\alpha_j r)}{\sqrt{r}},$$

where α_j's are the jth roots of $J_{n+\frac{3}{2}}(\alpha_j)=0$.

Corresponding to eqns. (21), (22) and (23), we have

$$(\lambda a^2+\kappa\alpha_j{}^2)\Theta_{n+1,j}^m-2\beta a(n+1)(n+2)S_{n+1,j}^m=0, \tag{47}$$

$$n(n+1)\lambda a^2T_{n,j}^m-2\Omega a^2\left\{\frac{n(n+2)(+m+1)}{2n+3}\alpha_jS_{n+1,j}^m+im\,T_{n,j}^m\right\}=0 \tag{48}$$

and

$$(n+1)(n+2)\alpha_j{}^2\lambda a^2S_{n+1,j}^m,-2\Omega a^2\left\{-\frac{n(n+2)(n+1-m)}{2n+1}\alpha_jT_{n,j}^m+im\alpha_j{}^2S_{n+1,j}^m\right\}$$
$$=r(n+1)(n+2)a^5\Theta_{n+1,j}^m. \tag{49}$$

From above three eqn. we get

$$\{n(n+1)\omega - im\kappa T\}\left\{(n+1)(n+2)\alpha_j{}^2 - im\alpha_j{}^2\kappa T - \kappa^2\frac{(n+1)^2(n+2)^2}{\omega+\kappa\alpha_j{}^2}R\right\}$$
$$+\frac{n^2(n+2)^2(n+n+1)(n+1-m)}{(2n+1)(2n+3)}\alpha_j{}^2\kappa^2T^2=0\,. \quad (50)$$

Eqn. (50) is reduced to

$$\omega^3+(p_1+ip_2)\omega^2+(q_1-R_1'+ip_1p_2)\omega+p_1q_1+i\frac{m\kappa T}{n(n+1)}R_1'=0\,, \quad (51)$$

where p_1, p_2 and q_1 are the same notations in (27); and $R_1'=\kappa^2\frac{(n+1)(n+2)}{\alpha_j{}^2}R$.

As eqn. (51) has the same form as eqn, (26), we can apply the examinations of eqn. (26) to eqn. (51). We have no steady state solutions.

i) axially symmetric solutions

In this case the discussion of [S_n, T_{n+1} ....] motion is entirely applicable; When $R_1>q_1$ we have an increasing amplitude instability, but when $R_1<q_1$, we get increasing amplitude oscillations and the critical frequency of oscillations is equal to that of [S_n, T_{n+1} ....] motion.

ii) asymmetric solutions

The real roots of eqn. (51) must satisfy the equations

$$x^3+p_1x^2+(q_1-R_1')x+p_1q_1=0, \quad (52)$$

and

$$p_2x^2+p_1p_2x+\frac{m\kappa T}{n(n+1)}R_1'=0. \quad (53)$$

The discussions of [S_n^m, T_{n+1}^m ....] motion is entirely applicable to [T_n^m, S_{n+1}^m....] motions, letting $n\to n-1$ and $R_1\to R_1'$. When

$$R_1'<q_1 \quad \text{and} \quad y>\frac{m\kappa T}{n(n+1)} \quad (54)$$

we have acase of overstability. The critical frequency of vibration is

$$\lambda=\frac{2}{n+1}\Omega\,. \quad (55)$$

Thus

$$\lambda\leqq\Omega \quad (56)$$

and tends to zero when n tends to infinity.

6. Concluding Remarks

We have found that thermal instability of rotating fluid sphere with negligible viscisity sets in as oscillations of increasing amplitude when R is smaller than a critical value. The critical frequencies of oscillations are smaller than the angular velocity of sphere. It is our results of this investigation that in a rotating fluid sphere with negligible viscosity the principle of the exchange of stabilities can not be applied and we have a case of overstability.

We are interested in the convection in the Earth's Core and in this case the effect of magnetic field can not be neglected. We shall discuss this problem further in the following paper.

7. Appendix

Equation of Motion [5], [7].

As we are seeking the effect of Coriolis force, we shall ignore the rotational flattening of the sphere in treating this problem. In the state of no convection, the temperature distribution, $T(r)$, is governed by

$$\frac{\partial T}{\partial t}=\kappa\nabla^2 T+\varepsilon=0 \quad , \tag{A1}$$

where κ is the coefficient of thermometric conductivity. The solution of eqn. (A.1) appropriate to the problem on hand is

$$T_0=\frac{\varepsilon}{6\kappa}(a^2-r^2)=\beta(a^2-r^2). \tag{A2}$$

We have assumed that $T_0=0$ at $r=a$; This entails no loss of generality.

If we assume the temperature distribution in the perturbed state

$$T=T_0+\theta, \tag{A3}$$

the equation govering θ is

$$\frac{\partial\theta}{\partial t}+(\boldsymbol{u}\cdot\nabla)T=\kappa\nabla^2\theta \ , \tag{A4}$$

where $\boldsymbol{u}$ denotes the velocity.

$$\rho\frac{\partial\boldsymbol{u}}{\partial t}+\rho(\boldsymbol{u}\nabla)\boldsymbol{u}=-\nabla P+\rho\nabla V+\rho\nu\nabla^2\boldsymbol{u}+\rho\boldsymbol{u}\times\boldsymbol{\Omega}, \tag{A5}$$

where ρ, P, V and ν denote density, pressure, gravitational potential and kinematic viscisity respectively.

Following Rayleigh [8], we shall allow in eqn. (A5) for the variation of density only is so far as it modifies the external field. Thus in eqn. (A.5) we shall replace ρ which occurs in front of ∇V by

$$\rho=\rho_0(1-\alpha T), \tag{A6}$$

where α denotes the coefficient of volume expansion and ρ_0 is the density at $r=a$ (where $T=0$) and regard ρ occuring elsewhere in eqn. (A.6) as ρ_0.

Now making use of relation (A.3), eqn. (A.5) becomes

$$\frac{\partial\boldsymbol{u}}{\partial t}+(\boldsymbol{u}\cdot V)\boldsymbol{u}=-\nabla\left(\frac{P}{\rho_0}-V\right)-\alpha\,[\beta(a^2-r^2)+\theta]\nabla V+\nu\nabla^2\boldsymbol{u}+2\boldsymbol{v}\times\boldsymbol{\Omega}. \tag{A7}$$

With variation of density due to thermal expansion allowed for in this manner, we shall treat u as a solenoidal vector

$$\operatorname{div}\boldsymbol{u}=0. \tag{A8}$$

Substituting the relation

$$\nabla V=-\frac{4}{3}\pi\bar{\rho}G\boldsymbol{r} \ , \tag{A9}$$

where G and $\bar{\rho}$ denote the constant of gravitation and mean density of the sphere, eqn. (A.7) becomes

$$\frac{\partial\boldsymbol{u}}{\partial t}+(\boldsymbol{u}\cdot\nabla)\boldsymbol{u}=-\nabla W+\gamma\theta\boldsymbol{r}+\nu\nabla^2\boldsymbol{u}+2\boldsymbol{u}\times\boldsymbol{\Omega}, \tag{A10}$$

where

$$\gamma=\frac{4}{3}\pi\bar{\rho}G\alpha \tag{A11}$$

and

$$W=\frac{\rho}{\rho_0}-V-\frac{1}{4}\beta\gamma(2a^2r^2-r^4). \tag{A12}$$

We shall suppose that $\boldsymbol{u}$ and θ are small quantities of the first order and that we can ignore products and squares of them.

Then, the equations in the perturbed state are

$$\frac{\partial\boldsymbol{u}}{\partial t}=-\nabla\frac{\delta p}{\rho}+\gamma\theta\boldsymbol{r}+\nu\nabla^2\boldsymbol{u}+2\boldsymbol{u}\times\Omega \tag{A13}$$

and

$$\frac{\partial\theta}{\partial t}=\kappa\nabla^2\theta+2\beta(rU_r), \tag{A14}$$

where δp is the perturbation in pressure.

Boundary Conditions

Boundary conditions which the solutions of eqns. (A.13) and (A.14) must satisfy depend on whether the bounding surface is rigid or free. but in all cases we requir that

$$\theta=0 \quad \text{and} \quad u_r=0 \text{ (on a bounding spherical surface).} \tag{A.15}$$

Additional boundary conditions follow from the equation of continuity and depend on the nature of the bounding surface.

Equation of continuity in spherical polar coordinates (r, ϑ, φ) is

$$\frac{\partial u_r}{\partial r}+2\frac{u_r}{r}+\frac{1}{r}\frac{\partial u_\vartheta}{\partial\vartheta}+\frac{u_\vartheta\cot\vartheta}{r}+\frac{1}{r\sin\vartheta}\frac{\partial u_\varphi}{\partial\varphi}=0, \tag{A16}$$

where u_r, u_ϑ and u_φ are the components of velocity along the principal elements of arc dr, $rd\vartheta$ and $r\sin\vartheta d\varphi$ respectively.

(i) on a rigid bounding surface

Acoording to eqn.(15) and (17) the conditions (A.15) require

$$\left.\begin{aligned}&S_n^m=0,\\ &\text{and}\\ &-n(n+1)a^2\frac{\partial}{\partial t}\frac{1}{r^2}\left\{\frac{d}{dr}\left(r^2\frac{d}{dr}\right)-n(n+1)\right\}\frac{S_n^m}{r}-\nu n(n+1)\left[\frac{1}{r^2}\left\{\frac{d}{dr}\left(r^2\frac{d}{dr}\right)\right.\right.\\ &\left.\left.-n(n+1)\right\}\right]^2\frac{S_n^m}{r}-2\Omega a^2\left[\frac{(n-1)(n+1)(n-m)}{2n-1}r^{n-1}\frac{d}{dr}(r^{-n-1}T_{n-1}^m)\right.\\ &\left.+\frac{n(n+2)(n+m+1)}{2n+3}r^{-(n+2)}\frac{d}{dr}(r^nT_{n+1}^m)-im\frac{1}{r}\left\{\frac{d^2}{dr^2}-\frac{n(n+1)}{r^2}\right\}S_n^m\right]=0,\\ &\text{on} \quad r=1.\end{aligned}\right\} \tag{A17}$$

As no slip occurs on the bounding surface, u_r, u_ϑ and u_φ must vanish. From eqns. (7), (16) and (A.16), it follows that

$$\left.\begin{aligned} &n(n+1)a^2\frac{\partial}{\partial t}\frac{T_n^m}{r^2}-\nu n(n+1)\frac{1}{r^2}\left\{\frac{d}{dr}\left(r^2\frac{d}{dr}\right)-n(n+1)\right\}\frac{T_n^m}{r^2}\\ &-2\Omega a^2\left[\frac{(n-1)(n+1)(n-m)}{2n-1}r^{n-1}\frac{d}{dr}(r^{-n}S_{n-1}^m)+\frac{n(n+2)(n+m+1)}{2n+3}r^{-(n+2)}\right.\\ &\qquad\left.\times\frac{d}{dr}(r^{n+1}S_{n+1}^m)\right]=0,\\ &\frac{dS_n^m}{dr}=0,\quad\text{and}\quad T_n^m=0\ \text{on}\ r=1. \end{aligned}\right\}\qquad(A18)$$

(ii) on a free bouding surface

In this case we must have in addition to the condition (A.17), the viscous stresses $P_{r\vartheta}$ and $P_{r\varphi}$ vanishes.

The expression for these stresses are

$$\left.\begin{aligned} P_{r\vartheta}&=\rho\nu\left(\frac{\partial u_r}{r\partial\vartheta}-\frac{u_\vartheta}{r}+\frac{\partial u_\vartheta}{\partial r}\right),\\ P_{r\varphi}&=\rho\nu\left(\frac{\partial u_r}{r\sin\vartheta\partial\varphi}-\frac{u_\varphi}{r}+\frac{\partial u_\varphi}{\partial r}\right) \end{aligned}\right\}\qquad(A19)$$

Since $\boldsymbol{u}_r$ vanishes on a bounding surface, the vanishing of $P_{r\vartheta}$ and$P_{r\varphi}$ requires

$$\frac{\partial u_\vartheta}{\partial\gamma}-\frac{u_\vartheta}{r}=\frac{\partial u_\varphi}{\partial r}-\frac{u_\varphi}{r}=0.\qquad(A20)$$

According to eqn. (7) these conditions are equivalent to

$$\frac{d}{dr}\left(\frac{1}{r}\frac{dS_n^m}{dr}\right)-\frac{1}{r^2}\frac{dS_n^m}{dr}=\frac{1}{r}\left(\frac{d^2S_n^m}{dr}-\frac{2}{r}\frac{dS_n^m}{dr}\right)=0$$

and

$$\frac{dT_n^m}{dr}=0\quad\text{on}\quad r=1.\qquad(A21)$$

Since $S_n^m=0$ on $r=1$, the first of (A.21) can be expressed as

$$\frac{\partial^2}{\partial r^2}\left(\frac{S_n^m}{r}\right)=0\quad\text{on}\quad r=1.\qquad(A22)$$

	Symbols
a	radius of sphere
G	Constant of gravitation
$\boldsymbol{i}_r$	unt vector of radius direction
p	pressure
T	temperature
$\boldsymbol{u}$	Velocity
V	Gravitational potential
α	Coefficient of volume expansion
$2\beta a$	temperature gradient at the boundary
γ	$\frac{4}{3}\pi\bar{\rho}G\alpha$
ε	the rate at which temperature would rise in the absence of conduction and conuection
θ	perturbation in temperature
κ	Coefficient of thermometric conductivity
ν	kinematic viscosity
ρ	density
Ω	angular velocity of sphere
$\boldsymbol{\omega}$	vorticity

8. Acknowledgements

The author wishes to express his sincere thanks to Prof. M. Hasegawa of Fukui University, Prof. Y. Tamura of Kyoto University, Prof. Y. Saito of Osaka City University and Dr. H. Miki for their continuous interest and encouragements in the course of this study and to Prof. K. Maeda of Kyoto University, Prof. T Nagata, Dr. T. Rikitake of Tokyo University, Dr. M. Hirono of Radio Research Laboratories and Dr. K. Nagashima of Nagoya University for their valuable discussions and advice on this problem.

References

[1] Chandrasekhar, S., Phil. Mag. 7 **43**, 501 (1952)
[2] Chandrasekhar, S., Proc. Roy. Soc., **217A**, 306 (1953)
[3] Chandrasekhar, S., **225A**, 173 (1954)
[4] Chandrasekhar, S., Proc. Roy. Soc., **237A**, 476 (1956)
[5] Chandrasekhar, S., Phil. Mag., 7 **43**, 1317 (1952)
[6] Takeuchi, H. and Shimazu, Y., Jurnal of Phys. of the Earth **2**, 73 (1954)
[7] Chandrasekhar, S., Phil. Mag., 7 **2**, 845 (1957)
[8] Rayleigh, Lord. Phil. Mag., 6 **32**, 529, Scientific Papess **6**, 432 (1916)
[9] Hide,R., Physics and Chemistry of the Earth, Pergamon Press (1956)

Fluid Motions in a Sphere II
Thermal Instability of a Conducting Fluid Sphere Heated within under a Uniform Magnetic Field

By Tomikazu NAMIKAWA

Institute of Politechnics, Osaka City University

(Read Oct. 9, 1957; Received July 20, 1958)

Abstract

In this paper the problem of thermal instability of non-viscous fluid sphere heated within under a uniform magnetic field is discussed. Differing from the former case of thermal instability of a rotating sphere, there exist axially symmetric steady state solutions and only (U_n^m, $V^m{}_{n+1}$, ...) motions can arise. Calculation suggests a relation between perturbations in magnetic field and vorticity. Under normal terrestrial conditions, instability arises as ordinary cellular convections, but under astrophysical conditions, it can arise depending on intensity of the uniform magnetic field, as cellular convections or as overstability, oscillations of increasing amplitude.

1. Introduction

In paper [I], we have examined thermal instability of a rotating fluid sphere and found that there is no steady state solutions; instability first sets in as overstability. We shall examine in this paper the influence of magnetic field on thermal convection in a sphere.

2. Equation of Motion

We shall consider a homogeneous conducting fluid sphere of radious a under a uniform magnetic field, the direction of which is taken to be z- axis. Assumption about the source of heat generation is the same as that of paper [I].

The equation of motion, of Maxwell, and of heat conduction appropriate to the problem on hand are

$$\rho\frac{\partial \boldsymbol{u}}{\partial t}+\rho(\boldsymbol{u}\cdot\nabla)\boldsymbol{u}=-\nabla P+\rho\nu\nabla^2\boldsymbol{u}+\rho\nabla V+\mu\boldsymbol{J}\times\boldsymbol{H}, \tag{1}$$

$$\operatorname{curl}\boldsymbol{H}=4\pi\boldsymbol{J}, \tag{2}$$

$$\operatorname{curl}\boldsymbol{E}=-\mu\frac{\partial \boldsymbol{H}}{\partial t}, \tag{3}$$

$$\operatorname{div}\boldsymbol{H}=0,\quad \operatorname{div}\boldsymbol{E}=4\pi c^2 q, \tag{4}$$

$$\boldsymbol{J}=\sigma(\boldsymbol{E}+\mu\boldsymbol{u}\times\boldsymbol{H}) \tag{5}$$

and

$$\frac{\partial T}{\partial t}+(\boldsymbol{u}\cdot\nabla)T=\kappa\nabla^2 T, \tag{6}$$

where $\boldsymbol{E}$, $\boldsymbol{J}$, $\boldsymbol{H}$, σ and μ denote the intensity of electric field, current density, intensity of magnetic field, electrical conductivity and the magnetic permeability. The meaning of other notations is equal to those in paper [I].

The equations governing small departures from the stationary state are (Appendix of [1]; [2])

$$\frac{\partial\theta}{\partial t}=\kappa\nabla^2\theta+2\beta(ru_r), \tag{7}$$

$$\frac{\partial\boldsymbol{u}}{\partial t}=-\frac{1}{\rho_0}\nabla P+\gamma\theta\boldsymbol{r}+\frac{\mu H}{4\pi\rho_0}\frac{\partial\boldsymbol{h}}{\partial z}+\nu\nabla^2\boldsymbol{u}, \tag{8}$$

$$\frac{\partial\boldsymbol{h}}{\partial t}=H\frac{\partial\boldsymbol{u}}{\partial z}+\eta\nabla^2\boldsymbol{h}, \tag{9}$$

and

$$\operatorname{div}\boldsymbol{u}=\operatorname{div}\boldsymbol{h}=0, \tag{10}$$

where H and $\boldsymbol{h}$ denote magnitude of uniform magnetic field and perturbation in magnetic field and

$$\eta=\frac{1}{4\pi\mu\sigma}. \tag{11}$$

Taking the curl of eqns. (8) and (9), we have

$$\frac{\partial\boldsymbol{\omega}}{\partial t}=\gamma\nabla\theta\times\boldsymbol{r}+\frac{\mu H}{4\pi\rho_0}\frac{\partial}{\partial z}\operatorname{curl}\boldsymbol{h}+\nu\nabla^2\boldsymbol{\omega}, \tag{12}$$

and

$$\frac{\partial}{\partial t}\operatorname{curl}\boldsymbol{h}=H\frac{\partial}{\partial z}\boldsymbol{\omega}+\eta\nabla^2(\operatorname{curl}\boldsymbol{h}). \tag{13}$$

Again, taking the curl of eqn. (12), we get

$$-\frac{\partial}{\partial t}\nabla^2\boldsymbol{u}=\gamma\ \operatorname{curl}(\nabla\theta\times\boldsymbol{r})-\frac{\mu H}{4\pi\rho_0}\frac{\partial}{\partial z}\nabla^2\boldsymbol{h}-\nu\nabla^4\boldsymbol{u}. \tag{14}$$

We can express the velocity field and the magnetic field as a superposition of a poloidal and a toroidal vector in terms of four scalars.

$$\boldsymbol{u}=\nabla V\times\boldsymbol{i}_r+\operatorname{curl}(\nabla U\times\boldsymbol{i}_r), \tag{15}$$

and

$$\boldsymbol{h}=\nabla T\times\boldsymbol{i}_r+\operatorname{curl}(\nabla S\times\boldsymbol{i}_r). \tag{16}$$

Five scalars U, V, T, S and θ are expressed as follows

$$\begin{aligned} U&=\sum_{n,m}U_n^m(r,t)Y_n^m, & V&=\sum_{n,m}V_n^m(r,t)Y_n^m,\\ S&=\sum_{n,m}S_n^m(r,t)Y_n^m, & T&=\sum_{n,m}T_n^m(r,t)Y_n^m, \end{aligned} \tag{17}$$

and

$$\theta=\sum_{n,m}\Theta_n^m(r,t)Y_n^m,$$

where Y_n^m is a surface spherical harmonic.

Multiplying eqns. (9), (12), (13) and (14) by r, we get

$$\frac{\partial(\gamma h_\gamma)}{\partial t}=H\boldsymbol{r}\frac{\partial \boldsymbol{u}}{\partial z}+\eta\nabla^2(rhr), \tag{18}$$

$$\frac{\partial}{\partial t}(r\omega r)=\frac{\mu H}{4\pi\rho_0}\boldsymbol{r}\frac{\partial}{\partial z}(\mathrm{curl}\,\boldsymbol{h})+\nu\nabla^2(r\omega_r), \tag{19}$$

$$\frac{\partial}{\partial t}r(\mathrm{curl}\,\boldsymbol{h})_r=H\boldsymbol{r}\frac{\partial}{\partial z}\boldsymbol{\omega}+\eta\nabla^2 r(\mathrm{curl}\,\boldsymbol{h})_r, \tag{20}$$

and

$$-\frac{\partial}{\partial t}\nabla^2(ru_r)=\gamma L^2\theta-\frac{\mu H}{4\pi\rho_0}\boldsymbol{r}\frac{\partial}{\partial z}\nabla^2\boldsymbol{h}-\nu\nabla^4(ru_r), \tag{21}$$

Operating Y_n^m to eqns, (7), (18), (19), (20) and (21) and expecuting the integration with respect to ϑ and φ, we get

$$a^2\frac{\partial}{\partial t}\Theta_n^m-\kappa\frac{1}{r^2}\left\{\frac{d}{dr}\left(r^2\frac{d}{dr}\right)-n(n+1)\right\}\Theta_n^m-2\beta an(n+1)\frac{U_n^m}{r}=0, \tag{22}$$

$$\begin{aligned}&a^2\frac{\partial}{\partial t}n(n+1)\frac{S_n^m}{r}-\eta n(n+1)\frac{1}{r^2}\left\{\frac{d}{dr}\left(r^2\frac{d}{dr}\right)-n(n+1)\right\}\frac{S_n^m}{r}\\&-Ha\left[\frac{(n-1)(n+1)(n-m)}{2n-1}r^{n-1}\frac{d}{dr}\{r^{-n}U_n^m\}+\frac{n(n+2)(n+m+1)}{2n+3}r^{-(n+2)}\right.\\&\left.\times\frac{d}{dr}(r^{n+1}U_{n+1}^m)+im\frac{Y_n^m}{r^2}\right]=0,\end{aligned} \tag{23}$$

$$\begin{aligned}&a^2\frac{\partial}{\partial t}n(n+1)\frac{V_n^m}{r^2}-\nu n(n+1)\frac{1}{r^2}\left\{\frac{d}{dr}\left(r^2\frac{d}{dr}\right)-n(n+1)\right\}\frac{V_n^m}{r^2}\\&-\frac{Ha}{4\pi\rho_0}\left[\frac{(n-1)(n+1)(n-m)}{2n-1}r^{n-1}\frac{d}{dr}(r^{-n}T_{n-1}^m)+\frac{n(n+2)(n+m+1)}{2n+3}r^{-(n+2)}\right.\\&\left.\times\frac{d}{dr}\left(r^{n+1}\frac{T_{n+1}^m}{r}\right)-\frac{im}{r}\left\{\frac{d^2}{dr^2}-\frac{n(n+1)}{r^2}\right\}S_n^m\right]=0,\end{aligned} \tag{24}$$

$$\begin{aligned}&-n(n+1)a^2\frac{\partial}{\partial t}\frac{1}{r^2}\left\{\frac{d}{dr}\left(r^2\frac{d}{dr}-n(n+1)\right)\right\}\frac{U_n^m}{r}+\nu n(n+1)\left[\frac{1}{r^2}\left\{\frac{d}{dr}\left(r^2\frac{d}{dr}\right)\right.\right.\\&\left.\left.-n(n+1)\right\}\right]^2\frac{U_n^m}{r}+\frac{\mu Ha}{4\pi\rho_0}\frac{1}{r^2}\left\{\frac{d}{dr}\left(r^2\frac{d}{dr}\right)-n(n+1)\right\}\left[\frac{(n-1)(n+1)(n-m)}{2n-1}\right.\\&\left.\times r^{n-1}\frac{d}{dr}(r^{-n}S_{n-1}^m)+\frac{n(n+2)(n+m+1)}{2n+3}r^{-(n+2)}\frac{d}{dr}(r^{n+1}S_{n+1}^m)+im\frac{T_n^m}{r^2}\right]\\&-\gamma n(n+1)a^5\Theta_n^m=0\end{aligned} \tag{25}$$

and

$$\begin{aligned}&a^2\frac{\partial}{\partial t}n(n+1)\frac{T_n^m}{r^2}-\eta n(n+1)\frac{1}{r^2}\left\{\frac{d}{dr}\left(r^2\frac{d}{dr}\right)-n(n+1)\right\}\frac{T_n^m}{r^2}\\&-Ha\left[\frac{(n-1)(n+1)(n-m)}{2n-1}r^{n-1}\frac{d}{dr}(r^{-n}V_{n-1}^m)+\frac{n(n+2)(n+m+1)}{2n+3}r^{-(n+2)}\right.\\&\left.\times\frac{d}{dr}(r^{n+1}V_{n+1}^m)-im\frac{1}{r}\left\{\frac{d^2}{dr^2}-\frac{n(n+1)}{r^2}\right\}U_n^m\right]=0.\end{aligned} \tag{26}$$

Eqns, (22), (23), (24), (25) and (26) are the basic equations of this problem.

3. Bouudary Conditions

As in [1], we shall discuss eqns. (24) and (25) neglecting the viscous term. We must require that

$$\Theta_n^m(1)=U_n^m(1)=0, \tag{27}$$

Additional boundary conditions are the continuity of magnetic field and tangential components of electric field on the boundary surface.

4. Solutions of Basic Equations

From eqns, (22), (23), (24), (25) and (26), we find that there exist groups of fluid motions and magnetic field as follows

$$\left.\begin{array}{llll} U_n^m \rightleftarrows V_{n+1}^m \rightleftarrows U_{n+2}^m \rightleftarrows & \cdots\cdots \\ \updownarrow \quad \updownarrow \quad \updownarrow & \\ T_n^m \rightleftarrows S_{n+1}^m \rightleftarrows T_{n+2}^m \rightleftarrows & \cdots\cdots \\ V_n^m \rightleftarrows U_{n+1}^m \rightleftarrows V_{n+2}^m \rightleftarrows & \cdots\cdots \\ \updownarrow \quad \updownarrow \quad \updownarrow & \\ S_n^m \rightleftarrows T_{n+1}^m \rightleftarrows S_{n+2}^m \rightleftarrows & \cdots\cdots \end{array}\right\} \tag{28}$$

We shall examine the $(U_n^m,\ T_n^m,\ V_{n+1}^m,\ S_{n+1}^m\ \ldots.)$ motions taking only the first four terms in considerations. Simple calculation shows that there is no $(V_n^m,\ U_{n+1}^m,\ S_n^m,\ T_{n+1}^m,\ \ldots.)$ motion because continuity of the magnetic field cannot be satisfied on the boundary surface. We expand $\dfrac{U_n^m}{r}$, $\dfrac{V_{n+1}^m}{r^2}$, $\dfrac{T_n^m}{r^2}$, $\dfrac{S_{n+1}^m}{r}$, and Θ_n^m as follows:

$$\left.\begin{array}{l} \dfrac{U_n^m}{r}=\sum_j U_{n,j}^m \dfrac{J_{n+\frac{1}{2}}(\alpha_j r)}{\sqrt{r}},\quad \dfrac{V_{n+1}^m}{r^2}=\sum_j V_{n+1,j}^m \dfrac{J_{n+\frac{3}{2}}(\alpha_j r)}{\sqrt{r}} \\ \dfrac{T_n^m}{r^2}=\sum_j T_{n,j}^m \dfrac{J_{n+\frac{1}{2}}(\alpha_j r)}{\sqrt{r}},\quad \dfrac{S_{n+1}^m}{r}=\sum_j S_{n+1,j}^m \dfrac{J_{n+\frac{3}{2}}(\alpha_j r)}{\sqrt{r}} \end{array}\right\} \tag{29}$$

and

$$\Theta_n^m=\sum_j \Theta_{n,j}^m \frac{J_{n+\frac{1}{2}}(\alpha_j r)}{\sqrt{r}},$$

where α_j's is the roots of $J_{n+\frac{1}{2}}(\alpha_j)=0$.

With above expressions, the boundary conditions (27) are satisfied.

The external magnetic field must satisfy eqns.

$$\operatorname{div} \boldsymbol{H}^e=0 \quad \text{and} \quad \operatorname{curl} \boldsymbol{H}^e=0 \tag{30}$$

and expressed as follows

$$\boldsymbol{H}^e=\nabla\psi, \tag{31}$$

where

$$\psi=\sum_{n,m} A_n^m r^{-(n+1)} Y_n^m(\vartheta, \varphi). \tag{32}$$

From eqns. (29), (31) and (32), it is found, after simple calculations, that the continuity of the magnetic field is satisfied on the boundary surface.

The internal electric field is given, from eqns, (2) and (5),

$$\boldsymbol{E}=\eta \operatorname{curl} \boldsymbol{H}-\mu \boldsymbol{u}\times \boldsymbol{H}. \tag{33}$$

Making use of eqn. (29), the internal electric field is calculated from eqn. (33).

The external electric field must satisfy eqns.

$$\operatorname{div} \boldsymbol{E}^e=0 \quad \text{and} \quad -\mu\frac{\partial \boldsymbol{H}^e}{\partial t}=\operatorname{curl} \boldsymbol{E}_e \tag{34}$$

and exprssed as follows:

$$\boldsymbol{E}^e=\sum\{B_n^m \nabla(r^{-(n+1)}Y_n^m)+C_n^m \nabla(r^{-(n+1)}Y_n^m)\}. \tag{35}$$

From eqns. (33), (34) and (35), it is found that the continuity of tangential components of electric field is satisfied.

If all quantities vary as $e^{\lambda t}$, substituting relations (29), eqns. (22), (23), (24), (25) and (26) are reduced to

$$(\lambda a^2+\kappa a_j^2)\Theta_{n,j}^m-2\beta a n(n+1)U_{n,j}^m=0, \tag{36}$$

$$(n+1)(n+2)\lambda a^2 V_{n+1,j}^m-\frac{Ha}{4\pi\rho_0}\left[-\frac{n(n+2)(n+1-m)}{2n+1}a_j T_{n,j}^m+ima_j^2 S_{n+1,j}^m\right]=0, \tag{37}$$

$$n(n+1)\lambda a^2 a_j^2 U_{n,j}^m-\frac{Ha}{4\pi\rho_0}a_j^2\left[\frac{n(n+2)(n+m+1)}{2n+3}a_j S_{n+1,j}^m+imT_{n,j}^m\right]$$
$$-rn(n+1)a^5\Theta_{n,j}^m=0, \tag{38}$$

$$(n+1)(n+2)(\lambda a^2+\eta a_j^2)S_{n+1,j}^m-Ha\left[-\frac{n(n+2)(n+1-m)}{2n+1}a_j U_{n,j}^m+im V_{n+1}^m\right]=0 \tag{39}$$

and

$$n(n+1)(\lambda a^2+a_j^2)T_{n,j}^m-Ha\left[\frac{n(n+2)(n+m+1)}{2n+2}a_j V_{n+1,j}^m+ima_j^2 U_{n,j}^m\right]=0. \tag{40}$$

From above eqns., we get

$$\left\{\omega^2+\eta a_j^2\omega+\frac{f_1}{(n+1)^2(n+2)}a_j^2\eta^2 Q\right\}\left[\omega^3+(\kappa+\eta)a_j^2\omega^2+\left\{\kappa\eta a_j^4+\frac{f_2}{n(n+1)^2}a_j^2\eta^2 Q\right.\right.$$
$$\left.\left.-\frac{n(n+1)}{a_j^2}\kappa\eta R\right\}\omega+\frac{f_2}{n(n+1)^2}\kappa\eta^2 a_j^4 Q-n(n+1)\kappa\eta^2 R\right]-4m^2$$
$$\times\frac{(n+1-m)(n+m+1)}{n(n+1)^2(n+2)(2n+1)(2n+3)}(a_j^2\eta^2 Q)^2(\omega+\kappa a_j^2)=0, \tag{41}$$

where

$$\left.\begin{aligned}&\omega=\lambda a^2,\quad Q=\frac{\mu^2 H^2\sigma a^2}{\rho_0\eta},\quad f_1=\frac{n(n+2)^2(n+m+1)(n+1-m)}{(2n+1)(2n+3)}+\frac{m^2}{n+2},\\&f_2=\frac{n(n+2)(n+m+1)(n+1-m)}{(2n+1)(2n+3)}+\frac{m^2}{n}\quad\text{and}\quad R=\frac{2\beta r a^6}{\kappa\eta}.\end{aligned}\right\} \tag{42}$$

5. Solutions of Marginal Stability

At first, assuming the validity of the principle of exchange of stabilities, we get the value of non dimensional number R of the marginal stabilities.

$$R_c^{\text{con}}=\left\{\frac{f_1^2}{n+1}-4m^2\frac{(n+m+1)(n+1-m)(n+1)}{(2n+1)(2n+3)f_1}\right\}\frac{a_j^4 Q}{n^2(n+1)^2} \tag{43}$$

As, for all value of n, the right hand side of (43) is negative, we have only axially

symmetric solutions of marginal stability, $[U_1^0, V_2^0, T_1^0, S_2^0, \cdots]$ motion, letting $m \to 0$ in (43).

Thus
$$R_c^{\text{con}} = \frac{(n+2)a_j^4 Q}{n(2n+1)(2n+3)(n+1)} = \frac{a_j^4 Q}{10}. \tag{44}$$

6. An Examination of the Principle of the Exchange of Stabilities

Here, we examine axially symmetric case of eqn. (41).

In this case eqn. (41) is reduced to
$$\omega^2 + \eta a_j^2 \omega + \frac{n(n+2)}{(2n+3)(2n+1)} a_j^2 \eta^2 Q = 0, \tag{45}$$

or
$$\omega^3 + (\kappa+\eta)a_j^2\omega^2 + \kappa\eta\left\{a_j^4 + \frac{(n+2)}{(2n+1)(2n+3)} a_j^2 Q \cdot \frac{\eta}{\kappa} - \frac{n(n+1)}{a_j^2} R\right\}\omega + \kappa\eta^2 a_j^2 \left\{\frac{(n+2)a_j^2}{(2n+1)(2n+3)} - \frac{n(n+1)}{a_j^2} R\right\} = 0. \tag{46}$$

Eqn. (45) has no real positive root, but eqn. (46) has real positive root if
$$\frac{n+2}{(2n+1)(2n+3)} a_j^2 Q < \frac{n(n+1)}{a_j^2} R, \tag{47}$$

and no real positive root if
$$\frac{n+2}{(2n+1)(2n+3)} a_j^2 Q > \frac{n(n+1)}{a_j^2} R \tag{48}$$

and
$$a_j^4 + \frac{(n+2)}{(2n+1)(2n+3)} a_j^2 Q \cdot \frac{\eta}{\kappa} - \frac{n(n+1)}{a_j^2} R > 0. \tag{49}$$

As eqn. (45) has no complex root with positive real part, we examine whether eqn. (46) has a complex root with positive real part under the condition (48) and (49).

We write eqn. (46) as follows:
$$\omega^3 + p\omega^2 + q\omega + r = 0, \tag{50}$$

where
$$\left.\begin{aligned} p &= (\kappa+\eta)a_j^2, \quad q = \kappa\eta\left\{a_j^4 + \frac{n+2}{(2n+1)(2n+3)} a_j^2 Q \cdot \frac{\eta}{\kappa} - \frac{n(n+1)}{a_j^2} R\right\} \\ \text{and} \quad r &= \kappa\eta^2 a_j^2 \left\{\frac{(n+2)}{(2n+1)(2n+3)} a_j^2 Q - \frac{n(n+1)}{a_j^2} R\right\}. \end{aligned}\right\} \tag{51}$$

If we put $\omega = x + iy$, where x and y are real numbers, eqn. (50) is reduced to
$$3x^2 + 2px + q = y^2 \tag{52}$$

and
$$x^3 + px^2 + qx + r - (3x+p)y^2 = 0. \tag{53}$$

From above two eqns. we have
$$8x^3 + 8px^2 + 2(p^2+r)x + pq - r = 0. \tag{54}$$

If

$$pq-r<0\,, \tag{55}$$

eqn. (54) admits a positive real root.

Thus if

$$q>0\,,\quad r>0\quad \text{and}\quad pq-r<0, \tag{56}$$

the principle of the exchange of stabilities can not be applied and we have a case of overstability.

According to eqn. (51), the condition (56) is equivalent to

$$\left(1+\frac{\eta}{\kappa}\right)a_j^4+\frac{(n+2)}{(2n+1)(2n+3)}a_j^2Q\left(\frac{\eta}{\kappa}\right)^2<\frac{n(n+1)}{a_j^2}R<a_j^4+\frac{(n+2)}{(2n+1)(2n+3)}a_j^2Q\cdot\frac{\eta}{\kappa}, \tag{57}$$

or

$$\left(1+\frac{\eta}{\kappa}\right)a_j^4+\frac{(n+2)}{(2n+1)(2n+3)}a_j^2Q\left(\frac{\eta}{\kappa}\right)^2<\frac{n(n+1)}{a_j^2}R<\frac{n+2}{(2n+1)(2n+3)}a_j^2Q\,, \tag{58}$$

according to whether

$$a_j^4+\frac{n+2}{(2n+1)(2n+3)}a_j^2Q\cdot\frac{\eta}{\kappa}<\frac{n+2}{(2n+1)(2n+3)}a_j^2Q\,, \tag{59}$$

or

$$a_j^4+\frac{n+2}{(2n+1)(2n+3)}a_j^2Q\cdot\frac{\eta}{\kappa}>\frac{n+2}{(2n+1)(2n+3)}a_j^2Q\,. \tag{60}$$

Rearranging the outer inequalities of (57) or (58), we get

$$0<a_j^4<\frac{n+2}{(2n+1)(2n+3)}a_j^2Q\left(1-\frac{\eta}{\kappa}\right), \tag{61}$$

or

$$0<\left(1+\frac{\eta}{\kappa}\right)a_j^2<\frac{n+2}{(2n+1)(2n+3)}a_j^2Q\left(1+\frac{\eta}{\kappa}\right)\left(1-\frac{\eta}{\kappa}\right). \tag{62}$$

These inequalities are the necessary conditions for the principle of exchange of stabilities not to be valid.

According to eqn. (61) or (62), a sufficient condition for the principle of exchange of stabilities to be valid is

$$\eta>\kappa\,. \tag{63}$$

This inequality is satisfied for the fiuid under terrestrial conditions (for example, mercury at room temperature) [2].

The frequency of oscillation at marginal stability is given by

$$\lambda=\frac{\sqrt{q}}{a^2} \tag{64}$$

and the critical value of R for the onset of convection is given by

$$R_c^0=\frac{(n+2)a_j^2Q}{n(n+1)(2n+1)(2n+3)}\left\{\left(\frac{\eta}{\kappa}\right)^2+\left(1+\frac{\eta}{\kappa}\right)\frac{a_j^2(2n+1)(2n+3)}{Q(n+2)}\right\}. \tag{65}$$

7. Onset of Instability in a Magnetic Field under Astrophysical Conditions

The inequality

$$\kappa \gg \eta \tag{66}$$

is characteristic of astrophysical conditions [2]. When (66) holds, the inequality (61) or (62) can be simplified to

$$Q > \frac{(2n+1)(2n+3)}{n+2} a_j^2 = Q_1 . \tag{67}$$

From eqn, (65), we can write for a considerable rarnge of Q satisfying (67),

$$R_c^0 = \frac{a_j^6}{n(n+1)} \quad \left(Q < \frac{\kappa^2}{\eta^2} Q_1 \right). \tag{68}$$

This is independent of the strength of the prevailing magnetic field. In axially symmetric case $n=1$ and minimum value of a_j is a_1: thus when (66) holds, instability in the form of oscillation of increasing amplitude can arise for

$$Q > 5 a_1^2 \tag{69}$$

and the critical value $\mathrm{R}^0{}_c$ remains practically constant and has the value

$$R_c^0 = \frac{a_1^6}{2} \quad \left(Q < \frac{\kappa^2}{\eta^2} 5 a_1^2 \right) \tag{70}$$

For $Q > \frac{k^2}{\eta^2} 5 a_1^2$, R_c^0 can be written

$$R_c^0 = R_c^{\mathrm{con}} \left(\frac{\eta}{\kappa} \right)^2, \tag{71}$$

where

$$R_c^{\mathrm{con}} = \frac{a_1^4}{10} Q . \tag{72}$$

On the other hand, if

$$Q < 5 a_1^2, \tag{73}$$

the principle of the exchange of stabilities will be applicable and instability sets in as the ordinary cellular convection. The critical value of R_c^{con} is given by eqn. (72) and it is less than that given by (70) so long as (73) holds. therefore we may say that for $Q < Q_1$ instability will arise by cellular convection while for $Q > Q_1$ it will arise through overstability.

According to eqns. (51) and (64), for $Q > Q_1$

$$\lambda \doteqdot \frac{a_1 \eta}{a^2} \sqrt{\frac{Q}{5}} \tag{74}$$

Magnetic field does not influence the critical value of R_c^0 (eqn. (70)), but does the frequency of oscillation with which overstability sets in. The meaning of this frequency becomes clearer when we express Q in terms of the velocity of the magneto-hydrodynamic wave [2].

$$V = \left(\frac{\mu H^2}{4\pi \rho_0} \right)^{\frac{1}{2}}. \tag{75}$$

From eqns. (11), (42) and (75)

$$Q=V^2\frac{a^2}{\eta^2}. \tag{76}$$

Thus we find

$$\lambda=\frac{a_1 V}{\sqrt{5}a}, \tag{77}$$

where $\frac{2\pi}{\lambda}$ is the time required for a magneto-hydrodynamic wave to travel a distance equal to $\frac{2\pi\sqrt{5}}{a_1}a$.

Letting

$$Q_1=5a_1^2=V_1^2\frac{a^2}{\eta^2}, \tag{78}$$

we get

$$V_1=\sqrt{5}\,a_1\frac{\eta}{a}. \tag{79}$$

Thus we may summerize that so leng as the velocity of magneto-hydrodynamic wave is less than V_1, instability will arise through cellular convection, but for $V_1<V<\sqrt{5}\,a_1\frac{\kappa}{a}$, we will have overstability when R^0 reaches the value given by (70).

8. Examinations of Onset of Instability in the General Case

Using eqns. (65) and (72) we can draw in the (R, Q)— plane the critical value of R. The convection curve starts on the R-axis at the point

$$R_c^{\text{con}}=0 \quad (Q=0) \tag{80}$$

and for $Q\to\infty$

$$R_c^{\text{con}}=\frac{a_1{}^4Q}{10} \quad (Q\to\infty). \tag{81}$$

On the other hand, the overstability curve starts on the R axis at

$$R_c^0=\frac{\left(1+\frac{\eta}{\kappa}\right)}{2}a_1{}^6 \quad (Q=0) \tag{82}$$

and for $Q\to\infty$ becomes asymptotic to the line

$$R_c^0=\frac{a_1{}^4Q}{10}\frac{\eta^2}{\kappa^2} \quad (Q\to\infty). \tag{83}$$

It follows that the overstability curve always starts above the convection curve.

i) From eqns. (81) and (83), it follows that the overstability curve lies entirely above the convection curve when

$$\eta\geqq\kappa. \tag{84}$$

In this case instability always arises as a cellular convection.

ii) According to Eqns. (81) and (83), when

$$\kappa>\eta, \tag{85}$$

the overstability curve intersects the convection curve and for $Q\to\infty$ lies below it. The

value of Q at the point where the two curves intersect is given by

$$Q_1' = \frac{5\alpha_1^2}{1-\frac{\eta}{\kappa}} = \frac{Q_1}{1-\frac{\eta}{\kappa}}. \tag{86}$$

Thus for $Q \leqq Q_1'$, instability arises as a cellular convection, but for $Q > Q'_1$, we shall have overstability when the critical value of R^0 is reached.

9. Concluding Remarks

It has been found that only (U_n^m, V_{n+1}^m, T_n^m, S_{n+1}^m, ...) motion can arise in a non- viscous sphere under a uniform magnetic field. The remarkable feature is that the order and degree of the spherical surface harmonics of perturbations in magnetic field and vorticity are equal. This may suggest a relation or resemblance between the magnetic field and vorticity, which is first proposed by Batchelor [3].

Under the normal terrestrial conditions ($\eta > \kappa$), the inhibition of convection by a magnetic field is a very pronounced effect, but under astrophysical conditions ($\kappa > \eta$), this is not. The results are quantitatively equal to those of Chandrasekhar's investigation of instability of a layer of fluid heated below under a uniform magnetic field. We shall treat the problem of instability of a fluid sphere under simultaneous action of rotation and magnetic field in the next paper.

10. Acknowledgements

The author wishes to express his sincere thanks to Prof. M. Hasegawa of Fukui University, Prof. Y. Tamura of Kyoto University Prof. Y. Saito of Osaka City University and Dr. H. Miki for their continuous interest and encouragement in the course of this study and to Pro. K. Maeda of Kyoto University, Prof. T. Nagata, Dr. T. Rikitake of Tokyo University, Dr. M. Hirono of Radio Research Laboratories and Dr. K. Nagashima of Nagoya University for their valuabe discussions and advice on this problem.

References

[1] Namikawa, T., J.G.G., **9**, 182 (1958)

[2] Chandrasekhar, S., Phil. Mag., 7, **43**, 501 (1952)

[3] Batchelor, G.K., Proc. Roy. Soc. **A 201**, 405 (1950)

Fluid Motions in a Sphere III
Thermal Instability of a Rotating Fluid Sphere Heated Within under a Uniform Magnetic Field

By Tomikazu NAMIKAWA

Institute of Politecnics, Osaka City University

(Read Oct. 9, 1957; Received July 20, 1958)

Abstract

The influence of simultaneous action of Corios force and magnetic field on convection in a non-viscus fluid sphere heated within is examined. It is found that there is only axially symmetric solutions of the marginal stability, and inhibition of convection by a magnetic field is pronounced when the intensity of magnetic field is larger than a critical value.

1. Introduction

In paper [1] and [2], we examined the influence of rotation and magnetic field on the thermal instability of fluid sphere heated within. We are interested in the origin of the earth's magnetic field and stellar magnetic field. According to the Elaasser-Bullard's dynamo theory of cosmic magnetic field, the maintenance of a magnetic field is induction effect in the earth's core or in the stars in which a thermal convection may exist. As the earth and the stars are rotating, we must solve the equation of fluid motion, of Maxwell and of heat conduction, taking into consideration Coriolis force.

As this is a very difficult problem, we treat in this paper, these equations in linearized form and examine the influence of a simultaneous action of magnetic field and rotation on the thermal instability of a fluid sphere heated within.

2. Equation of Motion

Consider a homogeneous conducting fluid sphere of radious a rotating with an angular velocity about z-axis under a uniform magnetic field, the direction of which is taken to be z-axis. Assumption about the source of heat generation is the same as that of paper [1] and [2]. The equation of motion, of Maxwell, and of heat conduction appropriate to the problem on hand are

$$\rho \frac{\partial \boldsymbol{u}}{\partial t} + \rho(\boldsymbol{u}\cdot\nabla)\boldsymbol{u} = -\nabla p + 2\rho \boldsymbol{u}\times\boldsymbol{\Omega} + \rho\nu\nabla^2\boldsymbol{u} + \rho\nabla V + \mu \boldsymbol{J}\times\boldsymbol{H}, \tag{1}$$

$$\text{curl } \boldsymbol{H} = 4\pi \boldsymbol{J}, \tag{2}$$

$$\text{curl } \boldsymbol{E}=-\mu\frac{\partial \boldsymbol{H}}{\partial t}, \tag{3}$$

$$\text{div } \boldsymbol{H}=0, \tag{4}$$

$$\text{div } \boldsymbol{E}=4\pi c^2 q, \tag{5}$$

$$\boldsymbol{J}=\sigma(\boldsymbol{E}+\mu\boldsymbol{u}\times\boldsymbol{H}), \tag{6}$$

and

$$\frac{\partial T}{\partial t}+(\boldsymbol{u}\cdot\nabla)T=\kappa\nabla^2 T. \tag{7}$$

The meaning of notations is equal to those in paper [1] and [2].

The equations governing small departures from the stationary state are ([1], [2], [3])

$$\frac{\partial\theta}{\partial t}=\kappa\nabla^2\theta+2\beta(ru_r), \tag{8}$$

$$\frac{\partial \boldsymbol{u}}{\partial t}=-\frac{1}{\rho_0}\nabla p+2\boldsymbol{u}\times\boldsymbol{\Omega}+\gamma\theta\boldsymbol{r}+\frac{\mu H}{4\pi\rho_0}\frac{\partial \boldsymbol{h}}{\partial z}+\nu\nabla^2\boldsymbol{u}, \tag{9}$$

$$\frac{\partial \boldsymbol{h}}{\partial t}=H\frac{\partial \boldsymbol{u}}{\partial z}+\eta\nabla^2\boldsymbol{h} \tag{10}$$

and

$$\text{div}\,\boldsymbol{u}=\text{div}\boldsymbol{h}=0. \tag{11}$$

Taking the curl of eqns. (9) and (10), we get

$$\frac{\partial\boldsymbol{\omega}}{\partial t}=\gamma\nabla\theta\times\boldsymbol{r}+2\Omega\frac{\partial \boldsymbol{u}}{\partial z}+\frac{\mu H}{4\pi\rho_0}\frac{\partial}{\partial z}\text{curl}\,\boldsymbol{h}+\nu\nabla^2\boldsymbol{\omega} \tag{12}$$

and

$$\frac{\partial}{\partial t}\text{curl}\,\boldsymbol{h}=H\frac{\partial}{\partial z}\boldsymbol{\omega}+\eta\nabla^2(\text{curl}\,\boldsymbol{h}). \tag{13}$$

Again, taking the curl of eqn. (12), we have

$$-\frac{\partial}{\partial t}\nabla^2\boldsymbol{u}=\gamma\,\text{curl}\,(\nabla\theta\times\boldsymbol{r})-\frac{\mu H}{4\pi\rho_0}\frac{\partial}{\partial z}\nabla^2\boldsymbol{h}-\nu\nabla^4\boldsymbol{u}. \tag{14}$$

We express the velocity field and the magnetic field as a superposition of a poloidal and a toroidal vector in terms of four scalars as in eqn. (15) and (16) of [2], and the four scalars are given in eqn. (17) of [2].

Multiplying eqns. (10), (12), (13) and (14) by $\boldsymbol{r}$, we get

$$\frac{\partial}{\partial t}(rhr)=H\boldsymbol{r}\frac{\partial \boldsymbol{h}}{\partial z}+\eta\nabla^2(rh_r), \tag{15}$$

$$\frac{\partial}{\partial t}(r\omega_r)=2\Omega\boldsymbol{r}\frac{\partial \boldsymbol{u}}{\partial z}+\frac{\mu H}{4\pi\rho_0}\boldsymbol{r}\frac{\partial}{\partial z}(\text{curl}\,\boldsymbol{h})+\nu\nabla^2(r\omega_r), \tag{16}$$

$$\frac{\partial}{\partial t}(\text{curl}\boldsymbol{h})_r=H\boldsymbol{r}\frac{\partial}{\partial z}\boldsymbol{\omega}+\eta\nabla^2 r(\text{curl}\boldsymbol{h})_r \tag{17}$$

and

$$-\frac{\partial}{\partial t}\nabla^2(ru_r)=\gamma L^2\theta+2\Omega\boldsymbol{r}\frac{\partial\boldsymbol{\omega}}{\partial z}-\frac{\mu H}{4\pi\rho_0}\boldsymbol{r}\frac{\partial}{\partial z}\nabla^2\boldsymbol{h}-\nu\nabla^4(rU_r). \tag{18}$$

Operating Y_n^m to eqns. (8), (15), (16), (17) and (18) and executing the integration with respect to ϑ and φ, we have

$$a^2\frac{\partial}{\partial t}\Theta_n^m-\kappa\frac{1}{r^2}\left\{\frac{d}{dr}\left(r^2\frac{d}{dr}\right)-n(n+1)\right\}\Theta_n^m-2\beta an(n+1)\frac{U_n^m}{r}=0, \tag{19}$$

$$n(n+1)a^2\frac{\partial}{\partial t}\frac{S_n^m}{r}-\eta n(n+1)\frac{1}{r^2}\left\{\frac{d}{dr}\left(r^2\frac{d}{dr}\right)-n(n+1)\right\}\frac{S_n^m}{r}$$
$$-Ha\left[\frac{(n-1)(n+1)(n-m)}{2n-1}r^{n-1}\frac{d}{dr}(r^{-n}U_n^m)+\frac{n(n+2)(n+m+1)}{2n+3}r^{-(n+2)}\right.$$
$$\left.\times\frac{d}{dr}(r^{n+1}U_{n+1}^m)+im\frac{V_n^m}{r^2}\right]=0, \tag{20}$$

$$a^2\frac{\partial}{\partial t}n(n+1)\frac{V_n^m}{r^2}-\nu n(n+1)\frac{1}{r^2}\left\{\frac{d}{dr}\left(r^2\frac{d}{dr}\right)-n(n+1)\right\}\frac{V_n^m}{r^2}$$
$$-2\Omega a^2\left[\frac{(n-1)(n+1)(n-m)}{2n-1}r^{n-1}\frac{d}{dr}(r^{-n}U_{n-1}^m)+\frac{n(n+2)(n+m+1)}{2n+3}r^{-(n+2)}\right.$$
$$\left.\frac{d}{dr}(r^{n+1}U_{n+1}^m)+im\frac{V_n^m}{r^2}\right]-\frac{\mu Ha}{4\pi\rho_0}\left[\frac{(n-1)(n+1)(n-m)}{2n-1}r^{n-1}\frac{d}{dr}(r^{-n}T_{n-1}^m)\right.$$
$$\left.+\frac{n(n+2)(n+m+1)}{2n+3}r^{-(n+2)}\frac{d}{dr}(r^{n+1}T_{n+1}^m)-\frac{im}{r}\left\{\frac{d^2}{dr^2}-\frac{n(n+1)}{r^2}\right\}S_n^m\right]=0, \tag{21}$$

$$-n(n+1)a^2\frac{\partial}{\partial t}\frac{1}{r^2}\left\{\frac{d}{dr}\left(r^2\frac{d}{dr}\right)-n(n+1)\right\}\frac{U_n^m}{r}+\nu n(n+1)\left[\frac{1}{r^2}\left\{\frac{d}{dr}\left(r^2\frac{d}{dr}\right)\right.\right.$$
$$\left.\left.-n(n+1)\right\}\right]^2\frac{U_n^m}{r}-2\Omega a^2\left\{\frac{(n-1)(n+1)(n-m)}{2n-1}r^{n-1}\frac{d}{dr}\left((r^{-n}V_{n-1}^m)\right)\right.$$
$$+\frac{n(n+2)(n+m+1)}{2n+3}r^{-(n+2)}\frac{d}{dr}(r^{n+1}V_{n+1}^m)-im\frac{1}{r}\left\{\frac{d^2}{dr^2}-\frac{n(n+1)}{r^2}\right\}U_n^m\Big]$$
$$+\frac{\mu Ha}{4\pi\rho_0}\frac{1}{r^2}\left\{\frac{d}{dr}\left(r^2\frac{d}{dr}\right)-n(n+1)\right\}\left[\frac{(n-1)(n+1)(n-m)}{2n-1}r^{n-1}\frac{d}{dr}(r^{-n}S_{n-1}^m)\right.$$
$$\left.+\frac{n(n+2)(n+m+1)}{2n+3}r^{-(n+2)}\frac{d}{dr}\left((r^{n+1}S_{n+1}^m)+im\frac{T_n^m}{r^2}\right]=\gamma n(n+1)a^5\Theta_n^m \right. \tag{22}$$

and

$$a^2n(n+1)\frac{\partial}{\partial t}\frac{T_n^m}{r^2}-\eta n(n+1)\frac{1}{r^2}\left\{\frac{d}{dr}\left(r^2\frac{d}{dr}\right)-n(n+1)\right\}\frac{T_n^m}{r^2}$$
$$-Ha\left\{\frac{(n-1)(n+1)(n-m)}{2n-1}r^{n-1}\frac{d}{dr}(r^nV_{n-1}^m)+\frac{n(n+2)(n+m+1)}{2n+3}r^{-(n+2)}\right.$$
$$\left.\frac{d}{dr}(r^{n+1}V_{n+1}^m)\frac{-im}{r}\left\{\frac{d^2}{dr^2}-\frac{n(n+1)}{r^2}\right\}U_n^m\right]=0. \tag{23}$$

Eqns. (19), (20), (21), (22) and (23) are the basic equations for this problem.

3. Boundary Conditions

As in [1] and [2], we shall treat eqns, (21) and (22) neglecting the viscous term.

The boundary conditions are the same as that of [2]. The vanishing of perturbation in temperature and radious component of velocity, and continuity of magnetic field and tangential components of electric field on the boundary surface are required.

4. Solutions of Basic Equations

As in [2], we shall examine the $(U_n^m, T_n^m, V_n^m, S_{n+1}^m..)$ motions taking only the first four terms in consideration. There is no $(V_n^m, S_n^m, U_{n+1}^m, T_{n+1}^m..)$ motion because the continuity of the magnetic field cannot be satisfied on boundary surface.

Expansions of velocity and magnetic field inside sphere or outside sphere, are equal to eqns. (29)–(35) of [2].

If all quatities mary like $e^{\lambda t}$, basic equations are reduced to

$$(\lambda a^2+\kappa\alpha_j^2)\Theta_{n,j}^m-2\beta an(n+1)U_{n,j}^m=0, \tag{24}$$

$$(n+1)(n+2)\lambda a^2V_{n+1,j}^m-2\Omega a^2\left[-\frac{n(n+2)(n+1-m)}{2n+1}\alpha_jU_{n,j}^m+imV_{n+1,j}^m\right]$$

$$-\frac{Ha}{4\pi\rho_0}\left[-\frac{n(n+2)(n+1-m)}{2n+1}\alpha_jT_{n,j}^m+im\alpha_j^2S_{n+1,j}^m\right]=0, \tag{25}$$

$$n(n+1)\lambda a^2\alpha_j^2U_{n,j}^m-2\Omega a^2\left[\frac{n(n+2)(n+m+1)}{2n+3}\alpha_jV_{n+1,j}^m+im\alpha_j^2U_{n,j}^m\right] \tag{26}$$

$$-\frac{Ha}{4\pi\rho_0}\alpha_j^2\left[\frac{n(n+2)(n+m+1)}{2n+3}\alpha_jS_{n+1,j}^m+imT_{n,j}^m\right]=\gamma n(n+1)a^5\Theta_{n,j}^m,$$

$$(n+1)(n+2)(\lambda a^2+\eta\alpha_j^2)S_{n+1,j}^m-Ha\left[-\frac{n(n+2)(n+1-m)}{2n+1}\alpha_jU_{n,j}^m+imV_{n+1,j}^m\right]=0, \tag{27}$$

$$n(n+1)(\lambda a^2+\eta\alpha_j^2)T_{n,j}^m-Ha\left[\frac{n(n+2)(n+m+1)}{2n+3}\alpha_jV_{n+1,j}^m+im\alpha_j^2U_{n,j}^m\right]=0. \tag{28}$$

From eqns. (24), (27) and (28), we obtain

$$\Theta_{n,j}^m=\frac{2\beta an(n+1)}{\lambda a^2+\kappa\alpha_j^2}U_{m,j}^n, \tag{29}$$

$$S_{n+1,j}^m=\frac{Ha\left[-\dfrac{n(n+2)(n+1-m)}{2n+1}\alpha_jU_{n,j}^m+imV_{n+1,j}^m\right]}{(n+1)(n+2)(\lambda a^2+\eta\alpha_j^2)} \tag{30}$$

and

$$T_{n,j}^m=\frac{Ha\left[\dfrac{n(n+2)(n+m+1)}{2n+3}\alpha_jV_{n+1,j}^m+im\alpha_j^2U_{n,j}^m\right]}{n(n+1)(\lambda a^2+\eta\alpha_j^2)}. \tag{31}$$

Substituting eqns. (29), (30) and (31) in eqns. (25) and (26), we get

$$\left[(n+1)(n+2)\omega-im\eta T+\frac{\alpha_j^2\eta^2Q}{(n+1)(\omega+\eta\alpha_j^2)}\left\{\frac{n(n+2)^2(n+1-m)(n+m+1)}{(2n+1)(2n+3)}\right.\right.$$

$$\left.\left.+\frac{m^2}{n+2}\right\}\right]V_{n+1,j}^m+\left[\frac{n(n+2)(n+1-m)}{2n+1}\alpha_j\eta T+\frac{2im\alpha_j^3\eta^2Q(n+1-m)}{(2n+1)(w+\eta\alpha_j^2)}\right]U_{n,j}^m=0 \tag{32}$$

and

$$\left[\frac{n(n+2)(n+m+1)}{2n+3}\alpha_j\eta T+\frac{2im\alpha_j{}^3\eta^2Q(n+m+1)}{(2n+3)(\omega+\eta\alpha_j{}^2)}\right]V^m_{n+1,j}$$
$$-\left[n(n+1)\alpha_j{}^2\omega-im\alpha_j{}^2\eta T+\frac{\alpha_j{}^4\eta^2Q}{(n+1)(\omega+\eta\alpha_j{}^2)}\left\{\frac{n(n+2)(n+m+1)(n+1-m)}{(2n+1)(2n+3)}\right\}\right.$$
$$\left.+\frac{m^2}{n}\right\}-\frac{n^2(n+1)^2}{(\omega+\kappa\alpha_j{}^2)}\kappa\eta R\left]U^m_{n,j}=0,\right. \tag{33}$$

where

$$\left.\begin{aligned}&\omega=\lambda a^2, \qquad T=\frac{2\Omega}{\eta}a^2, \quad Q=\frac{\mu^2H^2\sigma a^2}{\rho_0\eta}\\ \text{and}\qquad &R=\frac{2\beta\gamma}{\kappa\eta}a^6,\end{aligned}\right\} \tag{34}$$

From eqns. (32) and (33), we get

$$\left[(n+1)(n+2)\omega-im\eta T+\frac{f_1\alpha_j{}^2\eta^2Q}{(n+1)(\omega+\eta\alpha^{f2})}\right]\left[n(n+1)\omega-im\eta T+\frac{f_2\alpha_j{}^2\eta^2Q}{(n+1)(\omega+\eta\alpha_j{}^2)}\right.$$
$$\left.-\frac{n^2(n+1)^2\kappa\eta R}{\alpha_j{}^2(\omega+\kappa\alpha_j{}^2)}\right]+\frac{(n+1-m)(n+m+1)}{(2n+1)(2n+3)}\left[n(n+2)\eta T+\frac{2im\alpha_j{}^2\eta^2Q}{\omega+\eta\alpha^{f2}}\right]^2=0, \tag{35}$$

where

$$f_1=\frac{n(n+2)^2(n+1-m)(n+m+1)}{(2n+1)(2n+3)}+\frac{m^2}{n+2},$$

and

$$f_2=\frac{n(n+2)(n+m+1)(n+1-m)}{(2n+1)(2n+3)}+\frac{m^2}{n}. \tag{36}$$

Eqn. (35) is reduced to

$$\left[(n+1)(n+2)\omega^2+\eta\{(n+1)(n+2)\alpha_j{}^2-imT\}\omega+\eta^2\alpha_j{}^2\left\{\frac{f_1}{n+1}\cdot Q-imT\right\}\right]$$
$$\times\left[n(n+1)\omega^3+\kappa\left\{n(n+1)\left(1+\frac{\eta}{\kappa}\right)-imT\frac{\eta}{\kappa}\right\}\omega^2+\kappa\eta\alpha_j{}^2\left\{n(n+1)\alpha_j{}^2\right.\right.$$
$$+\frac{f_2}{n+1}Q\frac{\eta}{\kappa}-\frac{n^2(n+1)^2}{\alpha_j{}^4}R-imT\left(1+\frac{\eta}{\kappa}\right)\left.\right\}\omega+\kappa\eta^2\alpha_j{}^4\left\{\frac{f_2}{n+1}Q\right.$$
$$\left.\left.-\frac{n^2(n+1)^2}{\alpha_j{}^4}R-imT\right\}\right]+\frac{(n+1-m)(n+m+1)}{(2n+1)(2n+3)}(\omega+\kappa\alpha_j{}^2)\eta^2$$
$$\times[n(n+2)T\omega+n(n+2)\alpha_j{}^2\eta T+2im\alpha_j{}^2\eta Q]^2=0. \tag{37}$$

5. Solutions of Marginal Stability

Firstly we assume the validity of the principle of exchange of stabilities. Letting $w\to0$ in eqn. (37), we get then

$$\left\{\frac{f_1}{n+1}Q-imT\right\}\left\{\frac{f_2}{n+1}Q-\frac{n^2(n+1)^2}{\alpha_j{}^4}R-imT\right\}+\frac{(n+1-m)(n+m+1)}{(2n+1)(2n+3)}$$
$$\times\{n(n+2)T+2imQ\}^2=0. \tag{38}$$

This is reduced to

$$\left\{\frac{f_1f_2}{(n+1)^2}-4m^2\frac{(n+1-m)(n+m+1)}{(2n+)(2n+3)}\right\}Q^2+\left\{\frac{n^2(n+2)^2(n+1-m)(n+m+1)}{(2n+1)(2n+3)}\right.$$
$$\left.-m^2\right\}T^2-\frac{f_1}{n+1}Q\cdot\frac{n^2(n+1)^2}{\alpha_j{}^4}R=0 \tag{39}$$

and

$$R/Q=\left\{\frac{f_1+f_2}{n+1}-\frac{4n(n+2)(n+m+1)(n+1-m)}{(2n+1)(2n+3)}\right\}\frac{a_j^4}{n^2(n+1)^2}. \tag{40}$$

As the right hand side of eqn. (40) is negative for all value of $n(=m)$, we have no steady state solutions in general case.

Letting $m\to 0$ in (39), we get

$$R=\frac{a_j^4}{n^2(n+1)f_1}\left[\frac{f_1f_2}{(n+1)^2}Q+\frac{n^2(n+2)^2(n+1)^2}{(2n+1)(2n+3)}\frac{T^2}{Q}\right]. \tag{41}$$

We have only axially symmetric solutions of marginal stability, the $(U_1^0, V_2^0 \cdot T_1^0, S_2^0, \ldots)$ motion.

The minimum value of a_j is $a_1=4.5$; critical value of R is given by

$$R_c^{\text{con}}=a_1^4\left\{\frac{Q}{10}+\frac{5T^2}{Q}\right\}. \tag{42}$$

R_c^{con} has its minimum value when

$$Q=5\sqrt{2}\,T. \tag{43}$$

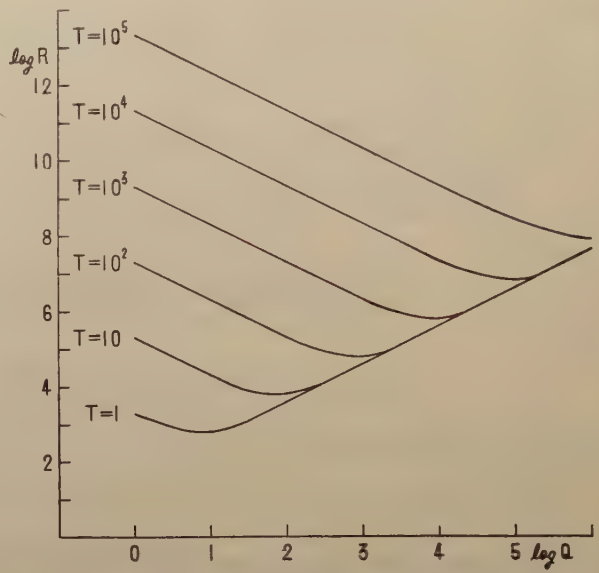

Dependence of the characteristic number R for the onset of convection on the number T and Q.

6. Concluding Remarks

It is found, from eqn. (42) that when angular velocity and other constant of fluid, κ, η, ρ, etc., are given, the inhibitation of convection by a magnetic field is pronounced only when intensity of magnetic field is larger than a critical value. The behaviour of R resembles to that of Chandrasekhar's investigation of instability of a layer of conducting fluid under simultaneous action of Coriolis force and uniform magnetic field.

We shall report in the near-future the results of the examination of non-steady state. It is supposed from the results of this paper that it is very interesting to investigate the convection in the earth's core, solving equations of motion, of Maxwell and of heat conduction in more complete way.

7. Acknowledgements

The author wishes to express his sincere thanks to Prof. M. Hasegawa of Fukui University, Prof. Y. Tamura of Kyoto University, Prof. Y. Saito of Osaka City University and Dr. H. Miki for their continuous interest and encouragements in the course of this study and to Prof. K. Maeda of Kyoto University, Prof. T. Nagata, Dr. T. Rikitake

of Tokyo University, Dr. M. Hirono of Radio Research Laboratories and Dr. K. Nagashima of Nagoya University for their valuable discussions and advices on this problem.

References

[1] Namikawa, T., J.G.G. **9,** 182 (1958)
[2] Namikawa, T., J.G.G. **9,** 193 (1958)
[3] Chandrasekhar, S., Proc. Roy. Soc., **A 225,** 173 (1954)

LETTERS TO THE EDITORS

The Result of Observation of the Rate of Ion Pair Production in the Atmosphere during the Solar Eclipse, Apr. 19, 1958.

The observation of the rate of ion pair production in the atmosphere near the ground has been carried out by the auther at Tanashi, Tokyo, from the view point of the atmospheric physics.

The instruments used for this observation are the ionization chamber and the vibrating reed electrometer. The form of the ionization chamber is a cylinder 90 cm long and 20 cm in radius having a volume of 27 liters. The wall of the chamber is myler of 7 micron thick (8.5×10^{-4} g/cm^2). The inner electrode, 5 mm in diameter, is supported centrally in the base of the chamber by a shielded insulator (teflon), and is connected to a vibrating reed electrometer (made by "Applied Physics" U.S.A.) by a shielded wire. The vibrating reed electrometer measures the saturated ionization current, to indicate the rate of ion pair production. The ionization chamber is set in the air flow cylinder. The air intake is placed at 1 m height from the ground surface.

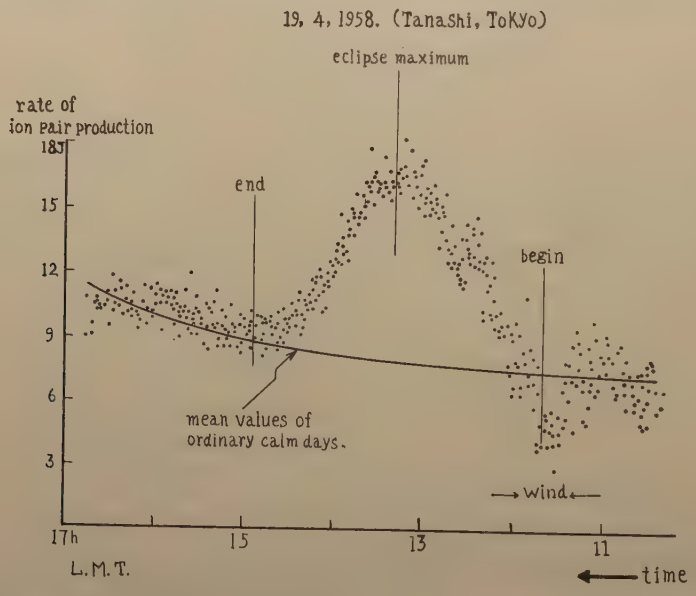

Figure shows the record of the rate of ion pair production during the solar eclipse of Apr. 19, 1958. In Tokyo, the solar eclipse was about 90 per cent of total. It was found that as the Sun's disk was obscured, the rate of ion pair production in the atmosphere immediately increased, again decreasing as the Sun came into view.

The value of the rate of ion pair production during the solar eclipse was larger than that of the other days. And, the maximum value occured at the time of the eclipse maximum, and is over twice of the value at the same time of the other days.

The detailed discussion on the result of observation mentioned above will be reported in the future.

By. M. KAWANO

Electrotechnical Laboratory, Tokyo, Japan.

On the Magnetic Field of S_d in the Middle and Lower Latitudes during the II Polar Year

1. Summary

The geomagnetic S_d field was calculated as the mean of five disturbed days in every month during the II polar year, by the same method which was adopted on the analysis of S_q [1], using the data of 45 observatories in the middle and lower latitudes.

Comparing this result with that of S_q calculated by H. Maeda, [2] S_D field was computed.

2. Brief Description of the Method

Using all available data, values of X components at the cross-points of parallel circles every 15° in latitudes and meridians every 30° in longitudes, the treatment was carried out about every two hours, i, e, 0^h, 2^h,……, 22^h LT, in order to obtain values in the mean state. Potential of S_d field of $\frac{1}{2}(S+W)$ was calculated through a method of graphical integration using the above X components. Values in latitude 60°N were nearly equal to values in latitude 60°N obtained from the analysis in polar region [3].

Potential V is expressed in the next equation.

$$V=r\sum P_n^m(\theta)\{A_n^m \cos l(T+\lambda)+B_n^m \sin l(T+\lambda)\}.$$

r: radius of the earth, T: universal time, λ: geomagnetic longitude $T+\lambda=t$: local time, $P_n^m(\theta)$: normalized function of *Ad.* Schmidt.

The value of A_n^m, B_n^m are indicated in Table I, In table II are indicated those of S_q obtained by H. Maeda [2].

Comparing these two Tables, it is found that the magnitude of amplitude is nearly equal and the comparatively large terms are A_2^1, A_4^1 A_3^2, A_4^3; B_2^1, B_4^1, B_3^2.

Table I. *The Coefficients of Sd. in Normalized force unit* 10^{-5} *c. g. s.*

	P_1^1	P_2^1	P_3^1	P_4^1	P_5^1	P_6^1
A_n^1	0.05	7.69	−0.24	−1.98	0.31	0.74
B_n^1	−0.16	−9.20	0.75	−1.57	0.42	−0.34
	P_2^2	P_3^2	P_4^2	P_5^2	P_6^2	P_7^2
A_n^2	0.34	−1.83	0.00	−0.80	−0.01	0.04
B_n^2	−0.28	−1.77	−0.10	0.23	−0.07	−0.47
	P_3^3	P_4^3	P_5^3	P_6^3	——	——
A_n^3	−0.13	1.06	−0.13	0.11	——	——
B_n^3	−0.02	−0.29	0.24	0.51	——	——

Taking the difference between the coefficients of S_d and S_q, we find the values of A_6^2, A_7^2, A_3^3, A_7^3, are very small and those of A_3^2, A_5^2, ;B_2^1, B_3^1, B_4^1, B_2^2, B_3^2 are comparatively large.

According to this table, it is seen that the diurnal and the semidiurnal terms predominate. From the values in Table III, the map of equipotential lines are drawn, which coincide nearly with that of S_D obtained by S. Chapman.

Table II. *The Coefficients of* S_q.

	P_1^1	P_2^1	P_3^1	P_4^1	P_5^1	P_6^1
A_n^1	−0.14	8.40	−0.63	−1.75	0.60	0.21
B_n^1	0.05	−2.35	−0.45	0.40	0.24	0.12
	P_2^2	P_3^2	P_4^2	P_5^2	P_6^2	P_7^2
A_n^2	0.00	−4.15	0.28	0.14	−0.07	−0.02
B_n^2	0.76	1.69	0.11	−0.15	0.09	0.22
	P_3^3	P_4^3	P_5^3	P_6^3	——	——
A_n^3	−0.09	1.42	−0.17	0.30	——	——
B_n^3	−0.54	−0.86	−0.04	−0.02	——	——

Table III. *The Coefficients of* S_d–S_q.

	P_1^1	P_2^1	P_3^1	P_4^1	P_5^1	P_6^1
A_n^1	0.19	−0.71	0.39	−0.23	−0.29	0.53
B_n^1	−0.21	−6.85	1.20	−1.97	0.18	−0.46
	P_2^2	P_3^2	P_4^2	P_5^2	P_6^2	P_7^2
A_n^2	0.34	2.32	−0.28	−0.94	0.06	0.06
B_n^2	−1.04	−3.46	−0.21	0.38	−0.16	−0.69
	P_3^3	P_4^3	P_5^3	P_6^3	——	——
A_n^3	−0.04	−0.38	0.04	−0.19	——	——
B_n^3	0.52	0.57	0.28	0.53	——	——

0.825×10^3 C.G.S.

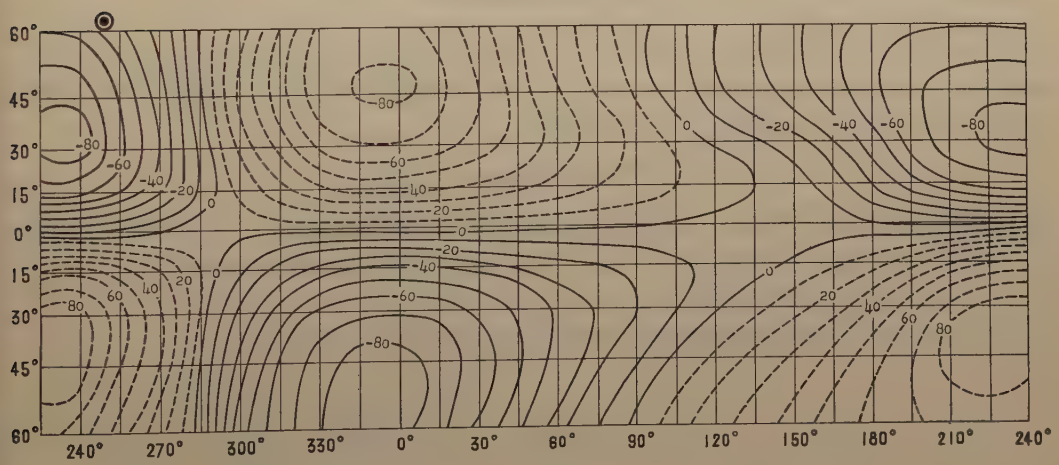

Fig. I. Equipotentials of the S_d field, where ◉ shows position of the Sun.

0.825×10^3 C.G.S.

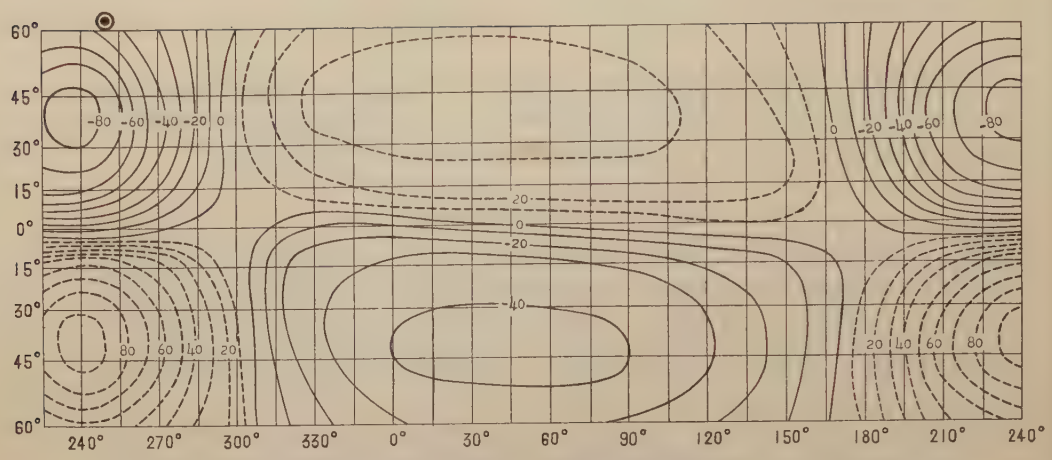

Fig. II. Equipotentials of the S_q field, where ◉ shows position of the Sun. [after H. Maeda]

0.825×10^3 C.G.S.

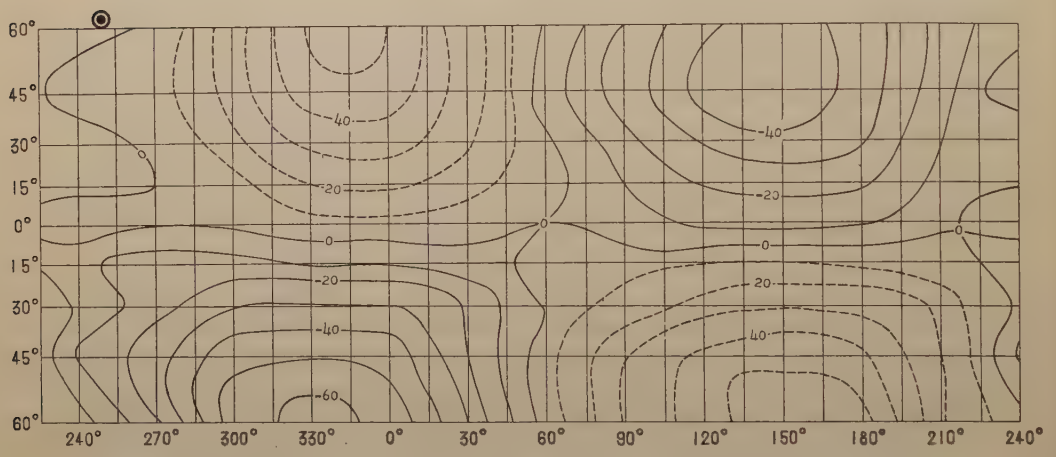

Fig. III. Equipotentials of the S_d—S_q field, where ◉ shows position of the Sun.

Acknowledgements

The author wishes to express his thanks to prof. M. Hasegawa for his kind direction and advice and to Dr. M. Ota, Dr. S. Matushita and Dr. H. Maeda for their guidance and help in the course of this work.

References

[1] M. Hasegawa and M. Ota. The Representation of magnetic field of S_q with the potential calculated through a method of graphical integration; Oslo Assembly, August 1948.

[2] H. Maeda, J.G.G. **5**, 39 (1953)

[3] M. Hasegawa, Transactions of Washington Meeting (IATME), 311 (1939)

Tomikazu NAMIKAWA

Institute of Politechnics, Osaka City University

Prevailing Wind in the Ionosphere and Geomagnetic S_q Variations

Recent observation of the wind motion in the ionosphere [1] has detected the considerably great velocity of the prevailing wind in the E region of the ionosphere. The prevailing wind in the ionosphere, as the zonal wind in the troposphere, is predominantly in the east-west direction and constant in local time.

The author derived the horizontal wind system in the E region from the geomagnetic S_q variations [2] [3]. In his calculation it was assumed that the wind motion corresponding to the S_q variation is periodic with local time. The prevailing wind motion, constant in local time, might make some contribution to the S_q current system due to the daily variations of the ionospheric conductivity. If the effect is noticeable, the treatment of the author would be based on the irrelevant assumptions and the results should be revised. The purpose of the present report is to show that the prevailing wind would play no role in the first-approximate treatment by which the previous calculations were carried out. In the first-approximation we assume that 1) the S_q current flows horizontally in the E region, which is a thin spherical shell, and 2) the geomagnetic field is that of a centered dipole alined along the geographical axis. Further the prevailing wind is assumed to be axisymmetric as the zonal wind in the troposphere [4]. Namely, the wind velocity $\boldsymbol{v}$ is

$$\left.\begin{aligned} u &\simeq 0 \quad , \\ v &= v(\theta) \ , \end{aligned}\right\} \tag{1}$$

where u is the southwards component, v the eastwards component of $\boldsymbol{v}$ and θ the colatitude. The eastwards component v is, in general, a function of θ. The electric field $\boldsymbol{E}$ is composed of the induced field and the static field as

$$\boldsymbol{E} = \boldsymbol{v} \times \boldsymbol{H} + \text{grad } S \ , \tag{2}$$

where $\boldsymbol{H}$ is the geomagnetic field, S the static potential. Ohm's law is given as

$$\boldsymbol{E} = [r]\boldsymbol{J} \ , \tag{3}$$

where $\boldsymbol{J}$ is the current density and $[r]$ the resistivity tensor defined as the reciprocal of the conductivity tensor $[\sigma]$ viz.

$$[\sigma] = \begin{pmatrix} \sigma_{xx} & \sigma_{xy} \\ -\sigma_{xy} & \sigma_{yy} \end{pmatrix} , \qquad [r] = [\sigma]^{-1} = \begin{pmatrix} r_{xx} & r_{xy} \\ -r_{xy} & r_{yy} \end{pmatrix} , \tag{4}$$

where

$$\left.\begin{aligned} r_{xx} &= \frac{\sigma_{yy}}{\sigma_{xx}\sigma_{yy} + \sigma_{xy}^2} \ , \\ r_{yy} &= \frac{\sigma_{xx}}{\sigma_{xx}\sigma_{yy} + \sigma_{xy}^2} \ , \\ r_{xy} &= -r_{yx} = \frac{-\sigma_{xy}}{\sigma_{xx}\sigma_{yy} + \sigma_{xy}^2} . \end{aligned}\right\}$$

In (4) an orthogonal x, y, and z coordinates are taken to be southwards, eastwards, and vertically upwards respectively. Next we transform the coordinates so that the x axis coincides withe the direction of $\boldsymbol{J}$. Then, by denoting the transformed quantities by a prime

$$[r']=\begin{pmatrix} \cos\alpha & \sin\alpha \\ -\sin\alpha & \cos\alpha \end{pmatrix}[r]\begin{pmatrix} \cos\alpha & -\sin\alpha \\ \sin\alpha & \cos\alpha \end{pmatrix}, \tag{5}$$

$$E'_x=\left[r_{xx}\cos^2\alpha+r_{yy}\sin^2\alpha\right]J'_x , \tag{6}$$

$$E'_y=\left[-(r_{xx}-r_{yy})\sin\alpha\cos\alpha-r_{xy}\right]J'_x , \tag{7}$$

where α is the angle between the x and x' axis. This angle is, of course, a function of θ and the longitude in general.

Now we take a line integration about a closed current path, provided that

$$\operatorname{div}\boldsymbol{J}=0 . \tag{8}$$

Then,

$$\oint_{\text{current}}\boldsymbol{E}d\boldsymbol{s}=\oint_{\text{current}}[r]\boldsymbol{J}d\boldsymbol{s} , \tag{9}$$

where $\boldsymbol{s}$ is the path of the electric current. By (2) and Stokes' theorem

$$\oint_{\text{current}}\boldsymbol{E}d\boldsymbol{s}=\oint_{\text{current}}(\boldsymbol{v}\times\boldsymbol{H})d\boldsymbol{s}=\iint\operatorname{rot}(\boldsymbol{v}\times\boldsymbol{H})d\boldsymbol{S} , \tag{10}$$

where the double integral means the integral over any regular surface bounded by $\boldsymbol{s}$. By (1)

$$(\operatorname{rot}\boldsymbol{v}\times\boldsymbol{H})_z=-\frac{1}{a\sin\theta}\frac{\partial}{\partial\lambda}\left[v(\theta)H_z\right] ,$$

where a is the radius of the earth, λ the longitude. From the assumptions 2)

$$H_z=-C\cos\theta , \tag{11}$$

where C is a constant.

Therefore

$$(\operatorname{rot}\boldsymbol{v}\times\boldsymbol{H})_z=0 , \tag{12}$$

and

$$\oint_{\text{current}}\boldsymbol{E}d\boldsymbol{s}=0 , \tag{13}$$

Accordingly (9) becomes

$$\oint_{\text{current}}[r]\boldsymbol{J}d\boldsymbol{s}=0 , \tag{14}$$

or by (6)

$$\oint_{\text{current}}(r_{xx}\cos^2\alpha+r_{yy}\sin^2\alpha)J'_x dx'=0 . \tag{14}'$$

As we integrate along the current path in the same direction as that of $\boldsymbol{J}$,

$$J'_x > 0 \ , \tag{15}$$

while

$$r_{xx} \cos^2 a + r_{yy} \sin^2 a > 0 \ . \tag{16}$$

Therefore

$$\boldsymbol{J} = 0 \ . \tag{17}$$

From the above argument it is concluded that the axisymmetric wind motion produces no electric current under any global distribution of the ionospheric conductivity in the dynamo theory, based on the above two assumptions, which have usually been made. The induced field is cancelled out by the resulting static field. Otherwise, free charges would accumulate constantly around the poles.

Actually, the two assumptions 1) and 2) would not exactly be met. The dependency of H_z on the longitude leads to production of a current by the axisymmetric wind motion. The prevailing wind actually contains a small southwards component which may give rise to a current flow. This has not been considered so far. Further, the 3-dimensional treatment will yield a different situation. However, these possibilities are likely to arise in the more detalied treatment, say, in the second order approximation. The outstanding character of the wind system corresponding to the S_q variations is represented in the results of our calculations [2] [3] [5] [6].

References

[1] W.G. Elford, Mixed Commission on the Ionosphere, New York, August (1957)
[2] S. Kato, J. Geomag. Geoelect., **8**, 24 (1956)
[3] S. Kato, J. Geomag. Geoelect., **9**, 107 (1957)
[4] C.G. Rossby, Bull. Amer. Met. Soc., **28**, 53 (1947)
[5] H. Maeda, J. Geomag. Geoelect., **7**, 121 (1955)
[6] H. Maeda, J. Geomag. Geoelect., **9**, 86 (1957)

Susumu KATO
Department of Electronics, Kyoto University

Meeting of the Society of Terrestrial Magnetism and Electricity:

The 23rd General Meeting was held at the Tokyo College of Science on may 17–19, 1958.

Number of the Reports read at the Meeting:

Rock Magnetism, 12; Atmospheric Electricity and Atmospherics, 8; Cosmic Rays, 10; Ionosphere, 11; Geomagnetism, 16; Earth Current, 2; Night Airglow, 3; Special Reports on Antarctic Research Expedition, 3.

JOURNAL OF GEOMAGNETISM AND GEOELECTRICITY

Vol. IX, 1957

INDEX OF AUTHORS

昭和33年 8 月29日　印刷
昭和33年 9 月 1 日　發行
第9卷　第4號

編輯兼發行者　日本地球電氣磁氣學會
代表者　長谷川万吉

印刷者　京都市南区上鳥羽唐戸町 63
田中幾治郎

賣捌所　丸善株式會社京都支店
丸善株式會社 東京・大阪・名古屋・仙台・福岡

JOURNAL OF GEOMAGNETISM AND GEOELECTRICITY

Vol. IX No. 4

1957

CONTENTS